

**A new seabed mobility index for the Irish Sea: Modelling seabed shear stress and classifying sediment mobilisation to help predict erosion, deposition, and sediment distribution.**

Coughlan, Mark; Guerrini, Marco; Creane, Shauna; O'Shea, Michael; Ward, Sophie; Van Landeghem, Katrien; Murphy, Jimmy; Doherty, Paul

**Continental Shelf Research**

DOI:

<https://doi.org/10.1016/j.csr.2021.104574>

Published: 01/11/2021

Publisher's PDF, also known as Version of record

[Cyswllt i'r cyhoeddiad / Link to publication](#)

*Dyfyniad o'r fersiwn a gyhoeddwyd / Citation for published version (APA):*

Coughlan, M., Guerrini, M., Creane, S., O'Shea, M., Ward, S., Van Landeghem, K., Murphy, J., & Doherty, P. (2021). A new seabed mobility index for the Irish Sea: Modelling seabed shear stress and classifying sediment mobilisation to help predict erosion, deposition, and sediment distribution. *Continental Shelf Research*, 229, [104574].

<https://doi.org/10.1016/j.csr.2021.104574>

**Hawliau Cyffredinol / General rights**

Copyright and moral rights for the publications made accessible in the public portal are retained by the authors and/or other copyright owners and it is a condition of accessing publications that users recognise and abide by the legal requirements associated with these rights.

- Users may download and print one copy of any publication from the public portal for the purpose of private study or research.
- You may not further distribute the material or use it for any profit-making activity or commercial gain
- You may freely distribute the URL identifying the publication in the public portal ?

**Take down policy**

If you believe that this document breaches copyright please contact us providing details, and we will remove access to the work immediately and investigate your claim.



# A new seabed mobility index for the Irish Sea: Modelling seabed shear stress and classifying sediment mobilisation to help predict erosion, deposition, and sediment distribution

Mark Coughlan<sup>a,b,c,\*</sup>, Marco Guerrini<sup>d</sup>, Shauna Creane<sup>c,e</sup>, Michael O'Shea<sup>d,e</sup>, Sophie L. Ward<sup>f</sup>, Katrien J.J. Van Landeghem<sup>f</sup>, Jimmy Murphy<sup>d,e</sup>, Paul Doherty<sup>c</sup>

<sup>a</sup> School of Civil Engineering, University College Dublin, Dublin, Ireland

<sup>b</sup> SFI Research Centre for Applied Geosciences (iCRAG), O'Brien Centre for Science East, University College Dublin, Dublin, Ireland

<sup>c</sup> Gavin and Doherty Geosolutions, Dublin, Ireland

<sup>d</sup> SFI Research Centre for Energy, Climate and Marine (MaRED), Beaufort Building, Environmental Research Institute, University College Cork, Ringaskiddy, Cork, Ireland

<sup>e</sup> School of Civil & Environmental Engineering, University College Cork, College Road, Cork, Ireland

<sup>f</sup> School of Ocean Sciences, Bangor University, Menai Bridge, Isle of Anglesey, LL59 5AB, UK

## ARTICLE INFO

### Keywords:

Sediment  
Mobilisation  
Disturbance  
Modelling  
Classification  
Irish sea

## ABSTRACT

The seafloor is increasingly being used for siting renewable energy and telecommunication infrastructure as well as supporting key fisheries and biodiversity. Understanding seabed stability and sediment dynamics is, therefore, a fundamental need for offshore engineering and geoscience and biological studies. In this study we aim to quantify the levels of sediment mobility in the Irish Sea: an area of increasing socio-economic interest and subsequent seabed pressures. The temporal and spatial interaction between bathymetry, hydrodynamics and seabed sediments leads to a complex pattern of erosion, bedload transport and deposition which can affect seabed infrastructure and modify habitats. Information on current and wave conditions were obtained from numerical modelling to assess their role in generating seabed hydrodynamic conditions. These outputs were coupled with observed seabed grain-size data to predict the exceedance of sediment mobility thresholds by bed shear stress values for a period of one year according to empirical formulae. Exceedance frequency values were used to calculate a number of sediment disturbance and mobility indexes to allow for a robust assessment of sediment dynamics. Sediment in the Irish sea, on average, is being mobilised 35% of the time during the year, with 35% of the spatial area studied being mobilised over 50% of the time. Even in areas of low sediment mobilisation frequency (<5%), there are implications for bedform dynamics. The spatial patterns of the calculated sediment mobility are discussed in the context of current seabed geomorphology and the implications for both engineering and environmental considerations.

## 1. Introduction

The seafloor supports a wide array of critical services that underpin our daily lives. Located between the Irish and British mainland, the Irish Sea is the focus of increasing socio-economic interest through the development of offshore renewable energy installations (the Irish Government is targeting 3 GW of offshore wind in the Irish Sea by 2030 (DCCA, 2019) as well as communications and energy infrastructure, such as the CeltixConnect cable and Greenlink interconnector. The Irish Sea is also home to a number of important fishing areas and contains a variety of benthic habitats as a result of its varied seafloor geology

(Kaiser et al., 1996; Robinson et al., 2011). The spatial and temporal interaction between hydrodynamical processes and seabed substrate has a profound influence on seafloor evolution with direct implications for a range of offshore activities such as marine engineering, renewable energy, and habitat mapping. Bed stresses induced by tidal currents, waves or a combination of both, can induce sediment mobility and bedload transport which can lead to erosion of the seabed, causing scour, or deposition of sediment causing burial. This fast-growing dependence on the seafloor demands better and forward-looking marine spatial planning and decision making at a range of scales (O'Higgins et al., 2019). This includes a firm understanding of the hydrodynamic processes that will

\* Corresponding author. School of Civil Engineering, University College Dublin, Dublin, Ireland.

E-mail address: [mark.coughlan@icrag-centre.org](mailto:mark.coughlan@icrag-centre.org) (M. Coughlan).

<https://doi.org/10.1016/j.csr.2021.104574>

Received 22 February 2021; Received in revised form 17 August 2021; Accepted 2 October 2021

Available online 5 October 2021

0278-4343/© 2021 The Authors. Published by Elsevier Ltd. This is an open access article under the CC BY license (<http://creativecommons.org/licenses/by/4.0/>).

affect seabed mobility in the future. Static substrate maps are typically available at regional resolution and do not take into account temporal variations in near-seafloor currents that can dramatically sculpt the seafloor by redistributing sediments, in turn exposing vulnerable infrastructure and modifying habitat type and extent. Substrate changes can exert many effects on habitats, across a range of spatial scales, including: (i) changing extent and distribution of the habitats and species; (ii) changing structure and function of the habitat; and (iii) changes in supporting processes on which the habitat relies (sediment suspension, different hydrodynamics due to different bed morphology etc.). More heterogeneous habitats support more species per unit area for instance (e.g. Tilman, 1982). Coarse gravel beds and rocks are linked to increased species richness, abundance and productivity (Bolam et al., 2010; Cooper et al., 2011) and can promote reefs and fish spawning. Natural disturbance of the seabed can often be exacerbated by anthropogenic impacts (e.g. trawling (Martín et al., 2015)) or can exacerbate anthropogenic input to the seafloor causing environmental issues (e.g. radionuclides and microplastics (Hunt and Kershaw, 1990; Martin et al., 2017)). A full understanding of present-day dynamics becomes even more important when considering the likely impacts of climate change to regional hydrography and metocean conditions (Olbert et al., 2012; Olbert and Hartnett, 2010).

A number of studies have established the hydrodynamics and sediment transport of the Irish Sea, including regional sediment transport pathways and localised phenomena such as bedload parting zones and a seasonal gyre in the western Irish Sea (Bowden, 1980; Hill et al., 1997; Holmes and Tappin, 2005; Pingree and Griffiths, 1979; Robinson, 1979; Van Landeghem et al., 2009). What is less well-understood is the relationship between near-bed hydrodynamics and sediment dynamics in terms of disturbance, mobilization and bedload transport. Ward et al. (2015) considered the relationship between simulated tidal-induced bed shear stress conditions and observed seabed sediment grain-size distribution. Whilst important in helping to understand seabed substrate distribution, it does not qualify other driving physical processes of sediment mobility in the Irish Sea (e.g. waves) or quantify sediment mobilisation levels on an annual basis. Wilson et al. (2018) modelled seabed disturbance for the northwest European shelf based on bed shear stress values exceeding a critical Shields threshold. Aggregated 1-day interval windows were used by Wilson et al. (2018) to classify disturbance events over monthly time periods at a regional scale ( $0.125^\circ \times 0.125^\circ$  resolution). The seabed stability model of Peters et al. (2020) used inferred values for critical bed shear stress ( $\tau_{cr}$ ) from mean reported values for individual sediment types based on a modified Folk classification, in combination with bathymetry and an inferred angle of repose. Estimated  $\tau_{cr}$  data from Peters et al. (2020) suggests a range of values for the Irish Economic Exclusion Zone (EEZ) including the Irish Sea but does not utilise any hydrodynamic information to infer sediment mobilisation.

The development of hydrodynamic and wave numerical models has allowed for the holistic computation of sediment mobilisation and transport due to currents and waves (e.g. Bever and MacWilliams, 2013; Dalyander et al., 2013). Sediment mobilisation can be assessed by using critical bed shear stress thresholds according to sediment grain-size and calculating how often these thresholds are exceeded by modelled bed shear stress induced by waves and/or currents according to well-established empirical formulae (e.g. Whitehouse, 1998). Typically, this is done for sediments which are non-cohesive in nature (Idier et al., 2010). A number of studies have used these shear stress threshold exceedance calculations to define regions of sediment mobilisation on the continental shelf based on the dominant hydrodynamic forcing and level of mobilisation frequency (Hemer, 2006; Porter-Smith et al., 2004). By developing standardised approaches to characterising sediment mobilisation based on the initial work of Porter-Smith et al. (2004) and Hemer (2006), Li et al. (2015) proposed three sediment mobility indices, which could be used universally on continental shelf settings, namely: a Mobilization Frequency Index (MFI), Sediment Mobility Index (SMI) and

Seabed Disturbance Index (SDI). These indices collectively consider not only the frequency of sediment threshold exceedance for mobilisation, but also the magnitude of disturbance events and have been successfully applied to localised, as well as shelf-scale, studies of the impact of hydrodynamic processes on sediment mobility (e.g. Joshi et al., 2017). In this study we apply the approaches proposed by Li et al. (2015) to develop a MFI, SMI and SDI for the Irish Sea and its approaches in order to consider the following: (1) the spatial variation of bed shear stress induced by currents, waves and a combination of both; (2) the frequency with which sediment mobility thresholds are exceeded by these hydrodynamic processes and the regional importance of each; (3) the magnitude of these events, and; (4) the implications of model results for seabed substrate distribution and morphodynamics. By doing so we aim to deliver evidence-based understanding (calibrated from local to regional scales in the Irish Sea) of sediment dynamics in the Irish Sea and a predictive guidance tool to enable decision making by a range of stakeholders.

## 2. Study area

Situated on the north-western European shelf, the Irish Sea is a semi-enclosed body of water between the Irish and British mainland (Fig. 1). Bed stresses in the Irish Sea are driven by a combination of water depth and the hydrodynamic regime, which is dominated by semi-diurnal tides (Pingree and Griffiths, 1979). The bathymetry of the Irish Sea consists of a central north-south trending trough, the Western Trough, which is nearly 100 km long and up to 150 m deep (Fig. 1). To the west and east of this trough are shallower, inner-shelf platforms which are generally <100 m water depth and consist of variable seabed morphologies, including sediment waves, sediment banks, enclosed deeps and sediment patches (Coughlan et al., 2020; Jackson et al., 1995; Mellet et al., 2015). The Western Trough links the St. Georges Channel to the south and the North Channel in the north. The ocean tide propagates from the North Atlantic onto the northwest European Shelf Sea and into the Irish Sea via St Georges Channel and, to a lesser extent, the North Channel, hence the tidal energy predominantly propagates south to north within the Irish Sea.

The wave climate in the Irish Sea is generally locally generated and usually consisting of waves that are short period and steep. Surface waves and storm surges are believed to have only a minor influence on regional bed stress patterns (Bowden, 1980). In the area west of the Isle of Man, seasonal solar heating induces thermal stratification causing density variations, which drives a cyclonic gyre forming during spring and summer (Hill et al., 1994; Horsburgh et al., 2000).

Having been previously glaciated, the seafloor sediment of the Irish Sea largely comprises reworked glacial or post-glacial material (Dobson et al., 1971; Holmes and Tappin, 2005; Jackson et al., 1995). These sediments form a range of grain-size classes, which are susceptible to becoming mobilised and redistributed (Ward et al., 2015). This mosaic of sediment types in the Irish Sea is primarily composed of sand- and gravel-grade material which dominates the central and southern part of the Irish Sea. Often these sediments exist as a thin veneer over more consolidated glacial units at, or near the surface (Jackson et al., 1995). In the north Irish Sea, west of the Isle of Man where seasonal stratification occurs, there is a large patch of muddy sediments referred to as the Western Irish Sea Mud Belt (WISMB). The sediments found here are mud-to sand-grade and can be up to 40 m in thickness (Belderson, 1964; Coughlan et al., 2019). Closer to shore and within the central Western Trough, there is a heightened expectancy of gravel-grade material or exposed bedrock to be present, most notably offshore Anglesey and the southern Irish coast. Mapping the seabed sediments of the Irish Sea has been carried out at various scales and made available by the British Geological Survey (BGS) as a 1:250,000 scale digital map product called DigSBS250. The database behind the map comprises grab sampling grabs of the top 0.1 m, combined with core and dredge samples, with the standard Folk triangle being used for sediment classification, which is

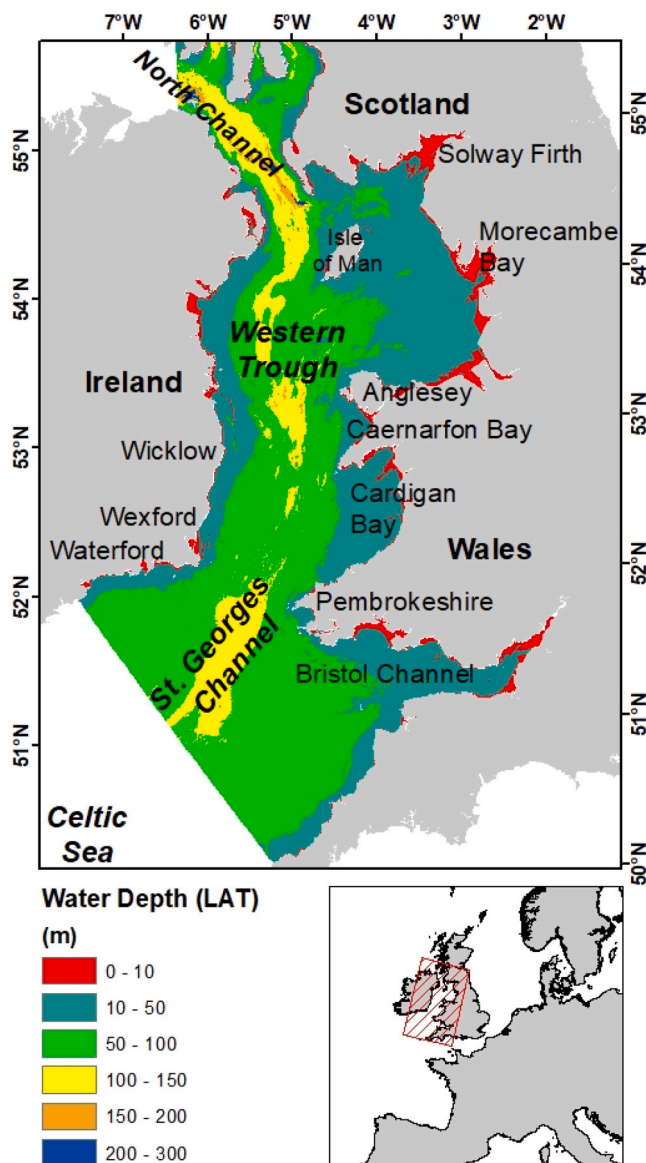


Fig. 1. Irish Sea bathymetry with water depth to lowest astronomical tide (LAT) within the study area and geographic locations mentioned in the text. Bathymetric metadata and Digital Terrain Model (DTM) data products have been derived from the EMODnet Bathymetry portal - <http://www.emodnet-bathymetry.eu>.

based on the percentage gravel and the sand:mud ratio (Folk, 1954).

For the purpose of this study, model boundaries were set extending from Magilligan Point in Northern Ireland to Islay in Scotland in the north, and from Ballycotton in Ireland to Land's End in England in the south (Fig. 1).

### 3. Materials and methods

Uncoupled Hydrodynamics (HD) and Spectral Waves (SW) models were developed in the DHI MIKE 21 suite of tools (DHI Group, 2017a; 2017b; 2017c; 2017d). The bathymetric data input to the models is described in section 3.1, with details of the HD and SW modelling strategy detailed in 3.2 and 3.3 respectively. Simulated outputs from these models consist of tidal water levels (surface elevation in m), current speed, significant wave height and wave period, which were validated using a combination of instrument measured datasets (see section 3.4). These simulated outputs were used to calculate bed shear stress

conditions due to current ( $\tau_c$ ), waves ( $\tau_w$ ) and combined current and wave ( $\tau_{cw}$ ) at 1-h time intervals over the course of a year (2019), producing a map of spatial variation across the study area (Fig. 1). This domain was divided into discrete points where calculations were performed of sediment mobility. A database of seabed sediment grain-size information, detailed in section 3.5, used in conjunction with bed shear stress conditions outputs allowed for the computing of a variety of sediment mobility indices, as outlined in section 3.6. These indices include calculating the mobilisation frequency as well as the levels of seabed disturbance and sediment mobilisation and have been adopted from Li et al. (2015).

#### 3.1. Bathymetry

Bathymetry was accessed from a combination of sources, including the European Marine Observation and Data Network (EMODnet) and the Integrated Mapping for the Sustainable Development of Ireland's Marine Resource (INFOMAR) programme. Regional data for the Irish Sea was derived from EMODnet data, which has a resolution of  $1/16 \times 1/16$  arc minutes (circa. 115 m grid) (EMODnet Bathymetry Consortium, 2018). In the Irish sector of the Irish Sea, these data were combined with higher resolution bathymetry data available through INFOMAR programme. Data were accessed through the INFOMAR Interactive Web Data Delivery System (IWDDS) and downloaded as individual raster datasets, mosaiced and used at a resolution of  $0.0005 \times 0.005^\circ$  (circa. 34 m  $\times$  55 m grid). INFOMAR data is levelled to their shallowest possible occurrence at lowest astronomical tide (LAT), according to a Vertical Offshore Reference Frame (VORF) datum. For model input the EMODnet data was kept referenced to Mean Sea Level (MSL) whereas INFOMAR data was converted from LAT to Malin ordnance datum (OD). The bathymetry was applied to the domain utilising a natural neighbour interpolation scheme. For the HD model the mesh element size varies from 2 km resolution at the open boundaries down to a minimum 10 m in areas where validation instruments are deployed (section 3.4). For the SW model the mesh element size varies from 2 km resolution at the open boundaries down to a minimum 200 m in areas where wave buoys are located (section 3.4).

#### 3.2. Hydrodynamic model

The MIKE 21 Flow Model FM Hydrodynamic (HD) Module is a 2-dimensional depth-averaged hydrodynamic programme that resolves the shallow water equations, or Navier Stokes Momentum, and continuity equations (Constantin and Foias, 1988; DHI Group, 2017c). These are resolved using a finite volume scheme. The Riemann solver (Roe, 1981) is used to determine the fluxes within the domain mesh, with various approximation schemes applied to resolve second order variance. The flow velocity is derived from the depth integrated resolution of the shallow water equations. Tide-induced bottom stresses are determined by a quadratic friction law which utilises drag coefficient and flow velocity. The simulated drag coefficient is calculated by resolving the Manning number (M) for bed friction (Manning et al., 1890). This model utilised a constant M-value for bed friction of  $32 \text{ m}^{1/3} \text{ s}^{-1}$  which was applied as a constant across the model domain. To drive the hydrodynamics a water surface elevation time series with a 15 min time interval was applied along both the north and south open boundaries of the domain, based on tidal constituents from the DHI Global Tide Model (DHI Group, 2019) with a spatial resolution of  $0.25^\circ \times 0.25^\circ$ . Model boundaries were set as fixed, but water level boundary conditions varied spatially along the boundary to represent the difference between the eastern and western sides of the Irish Sea. The astronomical constituents used to generate the boundary conditions included the major semidiurnal tidal constituents (M2, S2, N2 and K2) and diurnal (K1, O1, P1 and Q1). For validation and calibration, the simulated depth-averaged currents (magnitude and direction) and tidal elevation amplitudes were output at 10-min and 5-min intervals respectively

(section 3.4). For the calculation of bed shear stress and sediment mobility in section 3.6, outputs at 1-h intervals were utilised.

### 3.3. Wave model

Wave generation is simulated utilising the MIKE 21 Spectral Waves (SW) module (DHI Group, 2017d). The model can simulate both swell and locally generated waves. The wave action conservation equation (Komen et al., 1996) is resolved using an up-winding cell centered finite volume difference scheme. The model can include wind, swell, and non-linear wave to wave interaction as well as dissipation due to white capping, bottom friction, wave breaking, shoaling refractions and tidal elevations. White capping driven energy dissipation is based on the formulation of Bidlot et al. (2007). Dissipation due to bottom friction is computed using a constant friction factor (Komen et al., 1996), geometric roughness (Weber, 1991), and mobile bed-based approach (Johnson and Kofoed-Hansen, 2000). Depth induced wave breaking is calculated based on empirical formulations by Ruessink et al. (2003). Wave diffraction is modelled by the approximation of the mid-slope equation (Holthuijsen et al., 2003). The effect of wind forcing on the surface stress is incorporated into the model using empirical relationships that include density, drag coefficient and wind speed. The wind velocity 10 m above the surfaces is used as an input for this stress calculation. The wind and wave input data used in this model is from the European Centre for Medium-Range Weather Forecasts (ECMWF) ERA5 dataset, which is a 2-dimensional spatially varying hourly dataset. The wave generation was simulated by applying a time series of wave conditions at each boundary. The boundary condition comprised spectral wave height ( $H_{m0}$ ), peak wave period ( $T_p$ ), directional spreading and wave directions for both swell and wind-wave partitions of the wave

spectrum from the ERA5 dataset. As with the astronomical tidal boundary in the hydrodynamic model, the wave field varied along the boundary lines both at the north and south open boundary. A time and spatially varying 2D wind field was derived from the ERA5 dataset and over-imposed to the computational domain. To account for bed friction a Nikuradse roughness value (Nikuradse, 1933) of 0.04 m was applied as recommended by Weber (1991). The wave model outputs include significant wave height ( $H_s$ ),  $T_p$ , mean spectral wave zero-upcrossing period ( $T_{02}$ ), mean wave direction (MWD) and the near-bed horizontal orbital velocities ( $U_w$ ), which were output at 1-h intervals for both model validation (section 3.4) and the computation of the wave driven component of bed shear stresses for sediment mobility calculations (section 3.6).

### 3.4. Model validation

The hydrodynamic (HD) model was validated using coastal tide gauge data for water elevation and acoustic Doppler current profiler (ADCP) data for tidal current magnitude and direction (locations in Fig. 2). Data from tidal gauges on the Irish coast were accessed from the Marine Institute and on the British coast from the British Oceanographic Data Centre (BODC) and subsequently underwent a harmonic analysis to filter out the storm surge residual and enable a direct comparison with modelled tides. Pre-existing ADCP data were used here, acquired commercially from Irish consultancy Aquafact. Data from the M2 and M5 wave buoys were downloaded from the Met Éireann online delivery system. The comparisons between in-situ measurements and simulated predictions showed a good fit generally, with bias expressed as the mean difference between the observed data and simulated outputs. The correlation coefficient ( $R$ ) is a measure of the linear correlation between the

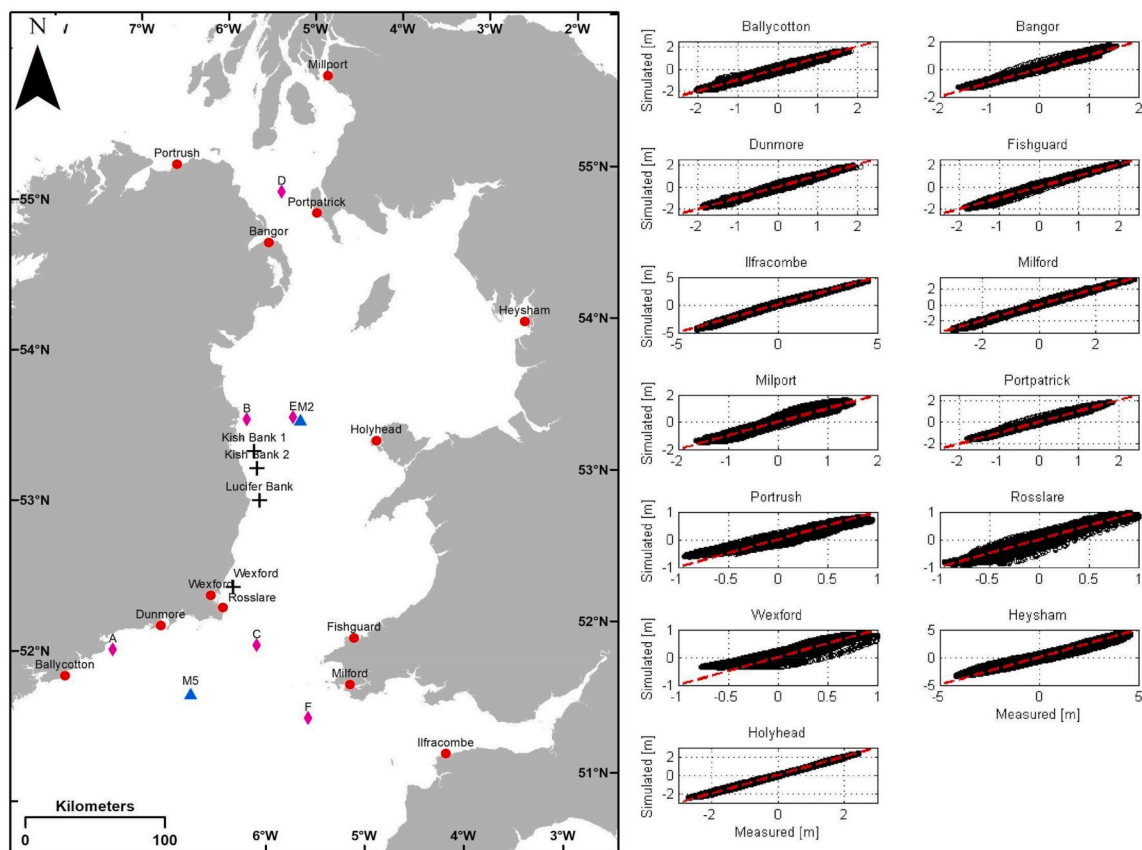


Fig. 2. Left panel: the locations of the tide gauge stations (red dots), offshore ADCPs (black crosses), grid points from the ERA5-ECMWF dataset (pink diamonds) and wave buoys (blue triangles) used in the model validation. Right panel: comparison between simulated and measured astronomical water level at various tide gauge stations.

observed data and simulated values. The scatter index (SI) takes the root mean square error (RMSE) of the difference between the observed data and simulated values and normalises the RMSE using the mean of the observed data.

Simulated water-levels were compared with timeseries from thirteen tidal gauges from around the Irish Sea from the period of May 01, 2019 to May 31, 2019 (Fig. 2). Overall, the comparisons showed a strong positive relationship with an average R value of 0.98 (Table 1).

Current measurements were taken at four locations in the Irish Sea using ADCP (Fig. 2). The ADCPs at these locations gathered data over non-synchronous time periods (Table 2). In general, the simulated values show good agreement with measured current speeds but tend to underestimate peak flood values (Fig. 3). A more significant discrepancy was noted in current direction, most notably in the Lucifer Bank dataset where there is a 30° shift in the major axis of the tidal ellipse between the measured and simulated value. Whilst no definite answer for this can be provided, it is attributed to issues with bathymetry resolution at the location creating a discrepancy in the simulated output.

Data used in the validation of wave parameters came from two sources. Initially, wave measurements taken at the M2 and M5 wave buoy locations were used for the 2019 period (Fig. 2). The model showed satisfactory comparisons with significant wave height from both buoys, with some discrepancy between simulated and measured values for wave period (T) and MWD (Fig. 4). However, it is important to note that this is not a like-for-like comparison, with the M2 and M5 buoys recording the wave period as  $T_s$ , or the significant wave period, whereas MIKE 21 calculates the wave period as the spectral zero crossing period ( $T_{02}$ ). Due to the short period of available concurrent measured data for the M2 and M5 buoys for the time frame considered, a model-to-model comparison was also carried out against the ERA5 dataset from the ECMWF to ensure a more robust validation. Grid point values from the ERA5-ECMWF dataset were compared to values at the same location from simulated outputs from this study (Fig. 4) and statistical comparisons were calculated (Table 3). Overall, this exercise provided a good comparison with an average R value of 0.97 across the six grid points chosen at random.

### 3.5. Seabed sediment data

Data characterizing seabed sediments were obtained from a number of public and academic sources, namely HabMap, the South West Irish Sea Survey (SWISS), the Irish Sea Aggregates Initiative (IMAGIN), Application of Seabed Acoustic Data in Fish Stocks Assessment and Fishery Performance (ADFISH), and data from the Joint Nature and Conservation Committee (JNCC) (for details on these see Ward et al. (2015) and references therein). Processed grab sample data from research surveys CV12007 (Van Landeghem et al., 2013) and CV09026 (Wheeler and shipboard party, 2009) were included along with

**Table 1**

Comparison between the simulated and observed tidal elevation amplitudes from tidal gauge location. The indices shown are bias, the root-mean-square error (RMSE), the correlation coefficient (R) and the scatter index (SI).

Location	Bias (m)	RMSE (m)	R	SI (%)
Ballycotton	-0.06	0.17	0.99	17.76
Bangor	-0.28	0.16	0.99	21.13
Dunmore	-0.23	0.14	0.99	15.22
Fishguard	-0.02	0.15	0.99	17.33
Ilfracombe	0.01	0.25	0.99	12.06
Milford	-0.02	0.17	1.00	11.40
Milport	-0.06	0.21	0.97	28.25
Portpatrick	-0.04	0.15	0.99	16.72
Portrush	-0.03	0.13	0.97	35.60
Rosslare	-0.01	0.13	0.97	31.71
Wexford	-0.09	0.18	0.94	49.30
Heysham	-0.07	0.59	0.97	27.68
Holyhead	0.02	0.12	1.00	9.73

**Table 2**

Comparison between the model and measured current data from ADCP locations. The indices shown are bias, the root-mean-square error (RMSE), the correlation coefficient (R) and the scatter index (SI).

Location	Data collection period	Bias (m/s)	RMSE (m/s)	R	SI (%)
Kish Bank 1	August 23, 2012 (12:50) - September 19, 2012 (11:20)	-0.03	0.08	0.89	26.28
Kish Bank 2	August 23, 2012 (15:00) - September 18, 2012 (05:10)	-0.07	0.13	0.88	32.96
Wicklow Trough	September 30, 2009 (01.40) - October 26, 2009 (09:50)	-0.08	0.21	0.83	32.14
Lucifer Bank	June 28, 2005 (01:30) - July 08, 2005 (11:10)	-0.04	0.11	0.85	29.61

processed grab sample data from the INFOMAR dataset. The entire dataset consists of 2318 analysed sediment grab samples (Fig. 5A). The samples were analysed using either wet sieving or laser diffraction. The raw data output of both methods were analysed in more detail using the GRADISTAT software to calculate grain-size statistics (Blott and Pye, 2001). These sample statistics are presented here using the graphical method according to Folk and Ward (1957). In particular, the median grain-size value (i.e.  $D_{50}$ ) was calculated for each sample location for use in sediment mobilization studies. Values ranged from 0.01 mm to 355 mm indicating medium-silt to boulder grade material, respectively (Fig. 5B).

Dense clustering of sediment samples in certain geographic locations is understandable given the focused and un-coordinated nature of the various surveys. Subsequently, the majority of samples are located within 25 km of the coastline. Similarly, large areas of the Irish Sea in this dataset have low to no sampling density. In order to help comparison with model output in areas where insufficient point sample data were available, a set of synthetic data points, complete with  $D_{50}$  values, were included from Wilson et al. (2018) (Fig. 5A). Whilst the Wilson et al. (2018) dataset represents synthetic values of grain-size, it is based on ground-truthing sediment sample data from a number of sources (e.g. INFOMAR and BGS) and uses rigorous geostatistical model approaches to interpolate the data into areas with fewer in-situ observational data. These models performed well in training tests (see Wilson et al., 2018).

### 3.6. Calculating sediment mobilisation

Sediments in shelf sea settings can be mobilised through the effects of currents, waves or by combined current and wave action. The primary acting mechanism is the frictional force exerted on the seabed by these phenomena, referred to as the bed shear stress ( $\tau_0$ ), which can be calculated by the following:

$$\tau_0 = \rho u_*^2 \quad (1)$$

where  $\rho$  is the density of water and  $u_*^2$  the frictional velocity. Outputs from both the 2D HD and SW models were used in this instance. Whilst it is accepted that 3D models provide more accurate results for calculating bed shear stress, 2D models have been shown to be comparable and requiring less computational time and resourcing (Glock et al., 2019). For non-cohesive sediments mobilisation occurs when the bed shear stress ( $\tau_0$ ) exceeds the critical bed stress ( $\tau_{cr}$ ). In the marine environment it is often convenient to relate the  $\tau_{cr}$  directly to the  $D_{50}$  where sediment characteristics data are available.

Van Rijn (1984) proposes a set of relationships, as part of the well-established Shields curve, between the dimensionless grain-size ( $D_*$ ) and the critical Shields parameter ( $\theta_{cr}$ ), which are expressed by the following formulae:

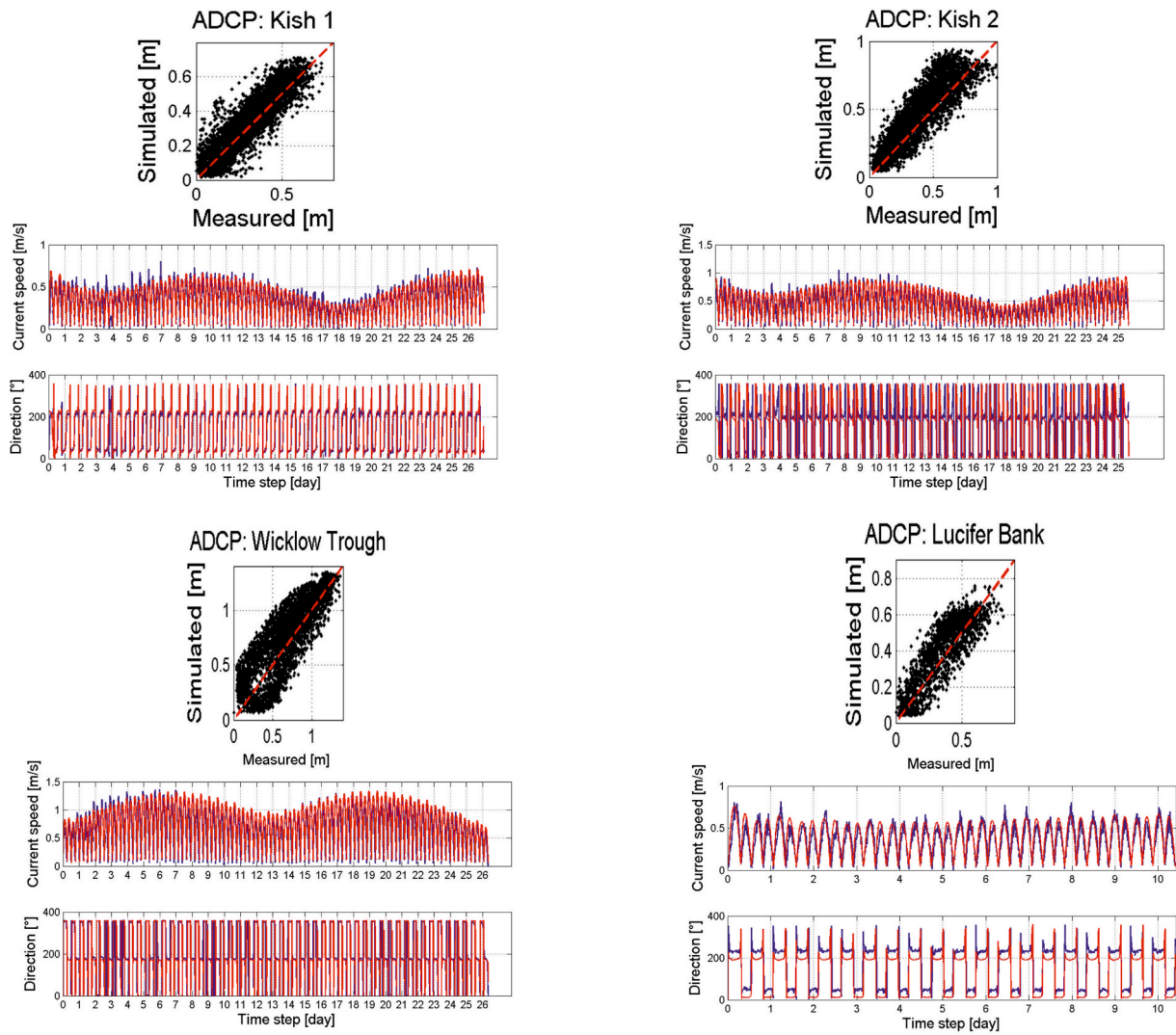


Fig. 3. Calibration profiles at each of the 4 ADCP locations in Fig. 2 for current speed and direction. Model simulated value is in red. Measured ADCP output is in blue.

$$D_* = D50 \left[ \frac{(s-1)g}{\nu^2} \right]^{1/3} \quad (2)$$

$$\theta_{cr} = \frac{u_{*,cr}^2}{(s-1)gD50} \quad (3)$$

where  $g$  is the gravitational acceleration,  $\rho_s$  is the grain density,  $\nu$  is the kinematic viscosity of water and  $s$  is the ratio of grain to water specific density ( $\rho_s/\rho$ ). By combining Equation (1) and Equation (3) it is possible to obtain the critical bed stress ( $\tau_{cr}$ ), which determines the threshold for sediment mobilisation:

$$\tau_{cr} = \theta_{cr}(\rho_s - \rho)gD50 \quad (4)$$

The conditions for sediment mobilisation require an understanding of the total shear stress acting upon the grain. In the marine environment the bed shear stress is often represented by the combined wave-current stress ( $\tau_{cw}$ ) generated by the non-linear interaction of current ( $\tau_c$ ) and wave ( $\tau_w$ ).

In this paper  $\tau_c$  and  $\tau_w$  are separately calculated and then combined. This enables the calculation of sediment mobilisation due to currents and waves as separate and combined effects. The current shear stress  $\tau_c$  acting upon a grain can be calculated by:

$$\tau_c = \rho C_D U^2 \quad (5)$$

where  $p$  is the water density,  $U$  the depth averaged current velocity and  $C_D$  is the dimensionless drag coefficient expressed by:

$$C_D = \left[ \frac{k}{\ln\left(\frac{h}{z_0}\right) - 1} \right]^2 \quad (6)$$

With  $k = 0.4$  being the Von Karman constant,  $h$  the local water depth described by the bathymetry and  $z_0$  the hydraulic roughness length which depends on the  $D50$  through:

$$z_0 = \frac{2.5 \cdot D50}{30} \quad (7)$$

The wave induced shear stress ( $\tau_w$ ) is calculated as:

$$\tau_w = 0.5 \rho f_w U_w^2 \quad (8)$$

where  $p$  is the water density,  $U_w$  is the amplitude of the horizontal bottom orbital velocity induced by the wave passage and  $f_w$  is the dimensionless wave friction:

$$f_w = 1.39 \left( \frac{1}{z_0} \frac{U_w T_p}{2\pi} \right)^{-0.52} \quad (9)$$

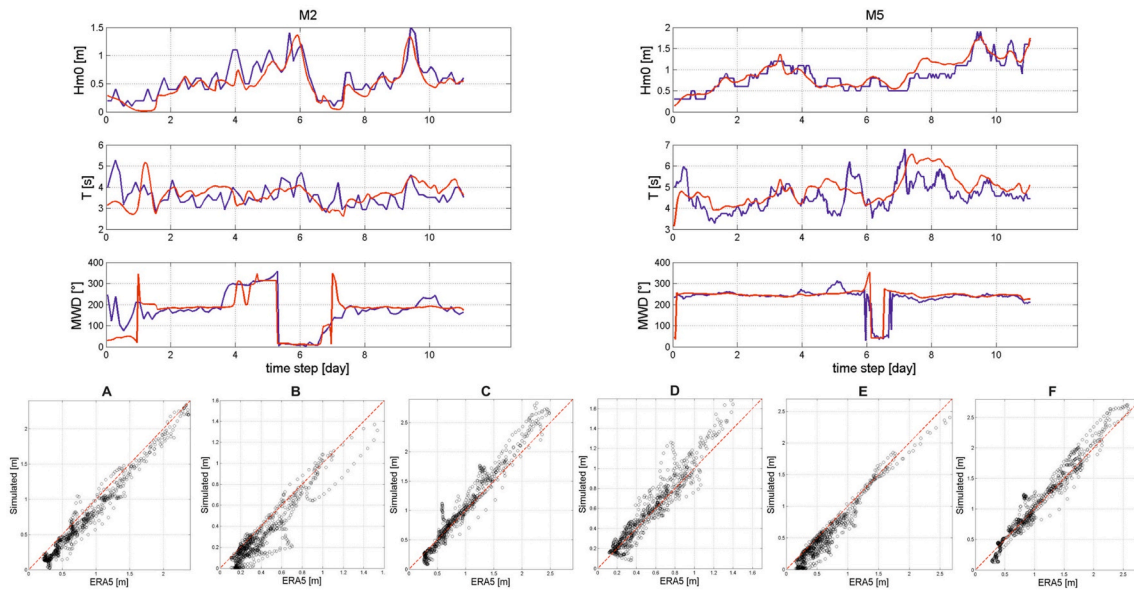


**Fig. 4.** Top left and right: Calibration profiles for wave data at M2 and M5 for spectral wave height (Hm0), wave period (referred to here as 'T' but expressed as Ts for measured wave buoy data and T02 for modelled output) and mean wave direction (MWD) . Model simulated value is in red and measured wave buoy output is in blue. Bottom panels show points derived from the ERA5-ECMWF dataset compared to simulated outputs (see Fig. 2 for locations).

**Table 3**

Comparison between the model and output from the ERA5-ECMWF dataset at locations shown in Fig. 2. The indices shown are bias, the root-mean-square error (RMSE), the correlation coefficient (R) and the scatter index (SI).

Location	Location	Significant Wave Height			
		Bias (m)	RMSE (m)	R	SI (%)
A	Lat: 52.0° Long: -7.5°	0.12	0.15	0.99	19.17
B	Lat: 53.5° Long: -6.0°	0.09	0.13	0.93	33.9
C	Lat: 52.0° Long: -6.0°	-0.06	0.17	0.98	18.24
D	Lat: 55.0° Long: -5.5°	-0.03	0.11	0.96	20.37
E	Lat: 53.5° Long: -5.5°	0.11	0.16	0.97	24.51
F	Lat: 51.5° Long: -5.5°	-0.03	0.14	0.98	13.11

With  $T_p$  being the wave spectral peak period and  $z_0$  as expressed by Equation (7).

With  $\tau_c$  and  $\tau_w$  calculated, the bed shear stress due to the non-linear combined effect of current and wave shear stresses is calculated using the following equation, as described in Whitehouse (1998):

$$\tau_{cw} = [(\tau_m + \tau_w \cos \varphi)^2 + (\tau_w \sin \varphi)^2]^{0.5} \tag{10}$$

where  $\varphi$  is the angle between the current speed and wave direction and  $\tau_m$  is derived from the formula:

$$\frac{\tau_m}{\tau_c} = 1 + 1.2 \left( \frac{\tau_w}{\tau_c + \tau_w} \right)^{3.2} \tag{11}$$

For calculating sediment mobility, sediment thresholds for mobilisation by bed shear stress, or the critical bed stress ( $\tau_{cr}$ ), were calculated using measured sediment values (D50) according to Equation (4). Computed stresses for  $\tau_{cw}$ ,  $\tau_c$  and  $\tau_w$  at each point in the domain of interest were compared to the corresponding  $\tau_{cr}$  value for that point to assess whether  $\tau_{cr}$  was exceeded. This frequency of threshold exceedance can be expressed as a percentage of the timeframe modelled (i.e. 1 year). Calculating the Mobilization Frequency Index (MFI) in this

manner is similar to the approach of Li et al. (2015) and reveals the frequency of mobilisation but not the strength. Alternatively, the combined bed shear stress for current and waves (i.e.  $\tau_{cw}$ ) highlights the magnitude of force acting on the seabed but contains no information on the effect of the magnitude in terms of sediment mobilisation. To better quantify seabed disturbance and mobilisation in the Irish Sea, a further set of indices were adopted from Li et al. (2015), who in turn developed them from the initial work of Hemer (2006). These include a Sediment Disturbance Index (SDI) and a Sediment Mobilisation Index (SMI). The SDI considers both the magnitude and frequency of force exerted on the seabed by disturbance events (in this case by combined waves and currents,  $\tau_{cw}$ ) and quantifies that force regardless of mobilisation. The approach to defining SDI adopted from Li et al. (2015) calculates index values at each grid point as the maximum value of the function  $(\tau_{cw})^{1.5P}$ , with P the point-dependant probability distribution of  $\tau_{cw}$ . The Sediment Mobilisation Index (SMI) calculates a non-dimensional value for the level of sediment mobility which incorporates both the magnitude and frequency of the event. Li et al. (2015) calculates the SMI as  $(\tau_{cw}/\tau_{cr}) \times (\% \text{ of } \tau_{cw} > \tau_{cr})$ , where  $\tau_{cw}/\tau_{cr}$  is calculated as the mean ratio of the values for when  $\tau_{cw}$  exceeds  $\tau_{cr}$ ; therefore, the larger the value of  $\tau_{cw}$  when it exceeds  $\tau_{cr}$  the higher the ratio.

#### 4. Results

The model outputs are for one year, 2019, with mean values calculated over that time. It is important to highlight that ‘maximum’ values presented here are maximum values for each data point location in the series and are not temporally synchronous.

##### 4.1. Tidal current velocities

The strongest mean values (1–1.5 m/s) are found in the North Channel (Fig. 6), whereas the rest of the Irish Sea generally shows values below 0.5 m/s with a mean value of 0.4 m/s. The strongest maximum values also occur in the North Channel (up to 3 m/s), although annual mean maximum values are around 1 m/s. Typically, low maximum values (<0.5 m/s) are noted in the areas of the Western Irish Sea Mud Belt (WISMB) and Eastern Irish Sea Mud Belt (EISMB) and in the Celtic Sea approach. These simulated current speeds were used to calculate bed shear stress values due to current ( $\tau_c$ ) according to Equation (5).



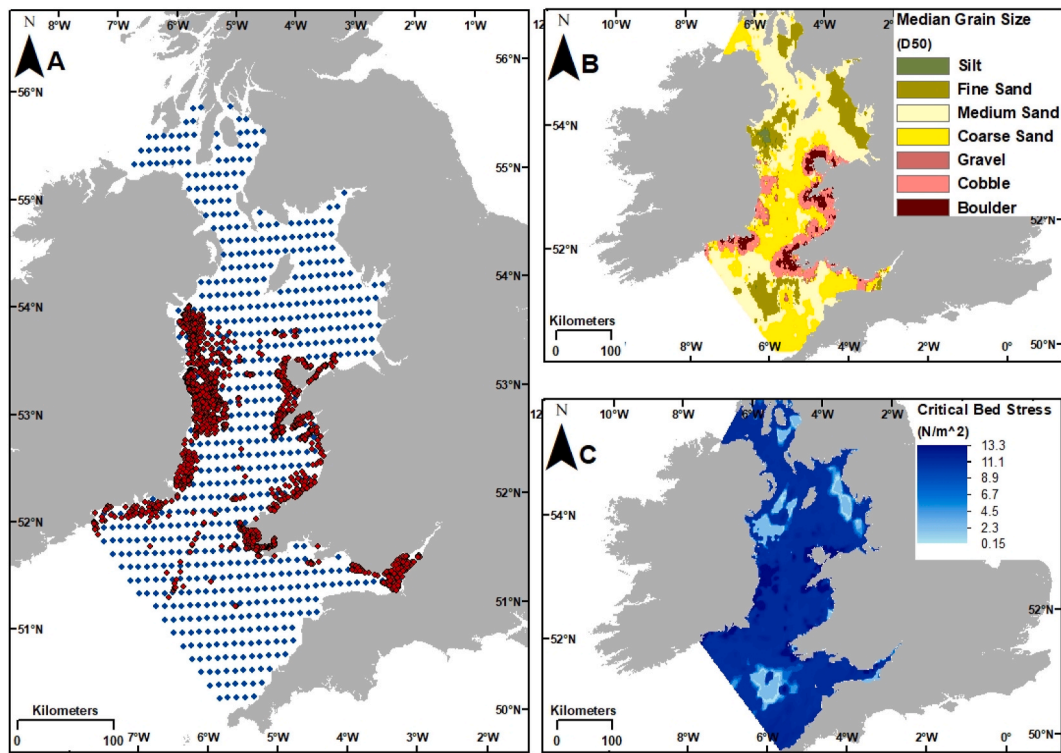


Fig. 5. A: Location of physical sediment samples (red points) and synthetic data points from Wilson et al. (2018) (blue points) used in this study for sediment characteristics. B: D50 (in mm) distribution based on sample distribution in left panel. C: Distribution of critical bed shear stress ( $\tau_{cr}$ ) based on D50 values.

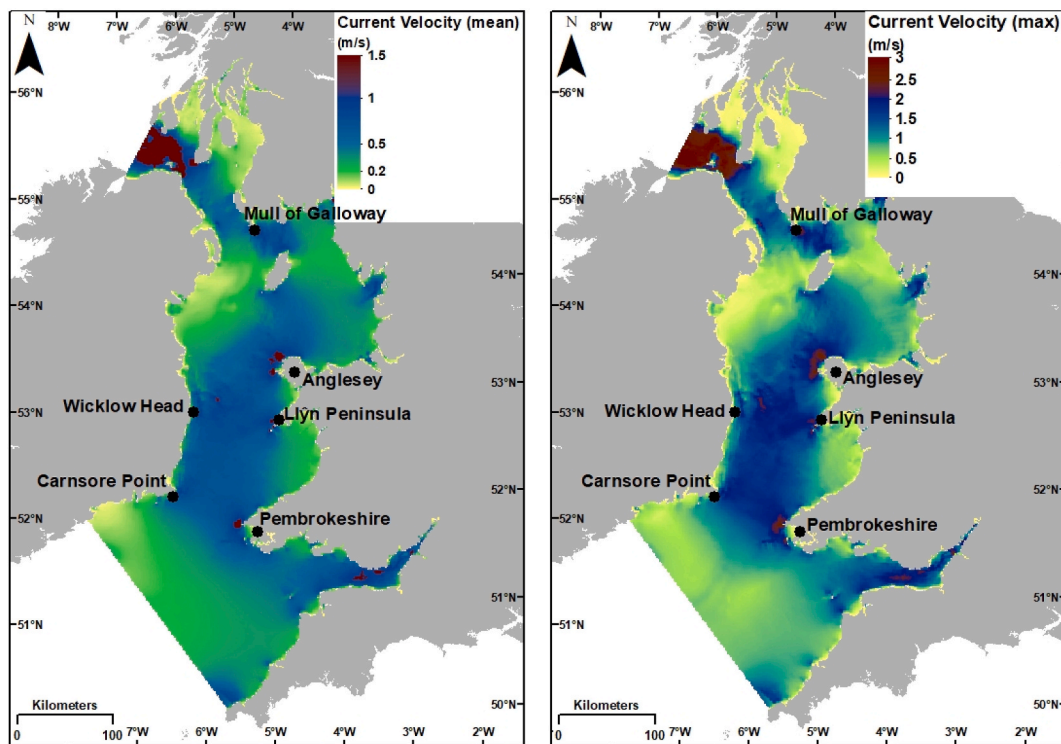


Fig. 6. Maps of depth-averaged current velocities in metres per second (m/s). Left panel displays mean values and the right panel displays maximum values. Additional locations mentioned in the text are highlighted.

4.2. Waves

Wave height and period are highest in the North Channel and St.

George’s Channel, decreasing towards the central Irish Sea (Fig. 7). In general, values agree with simulated output from other sources. For example, annual mean  $H_s$  values of 1 m approximately reported by

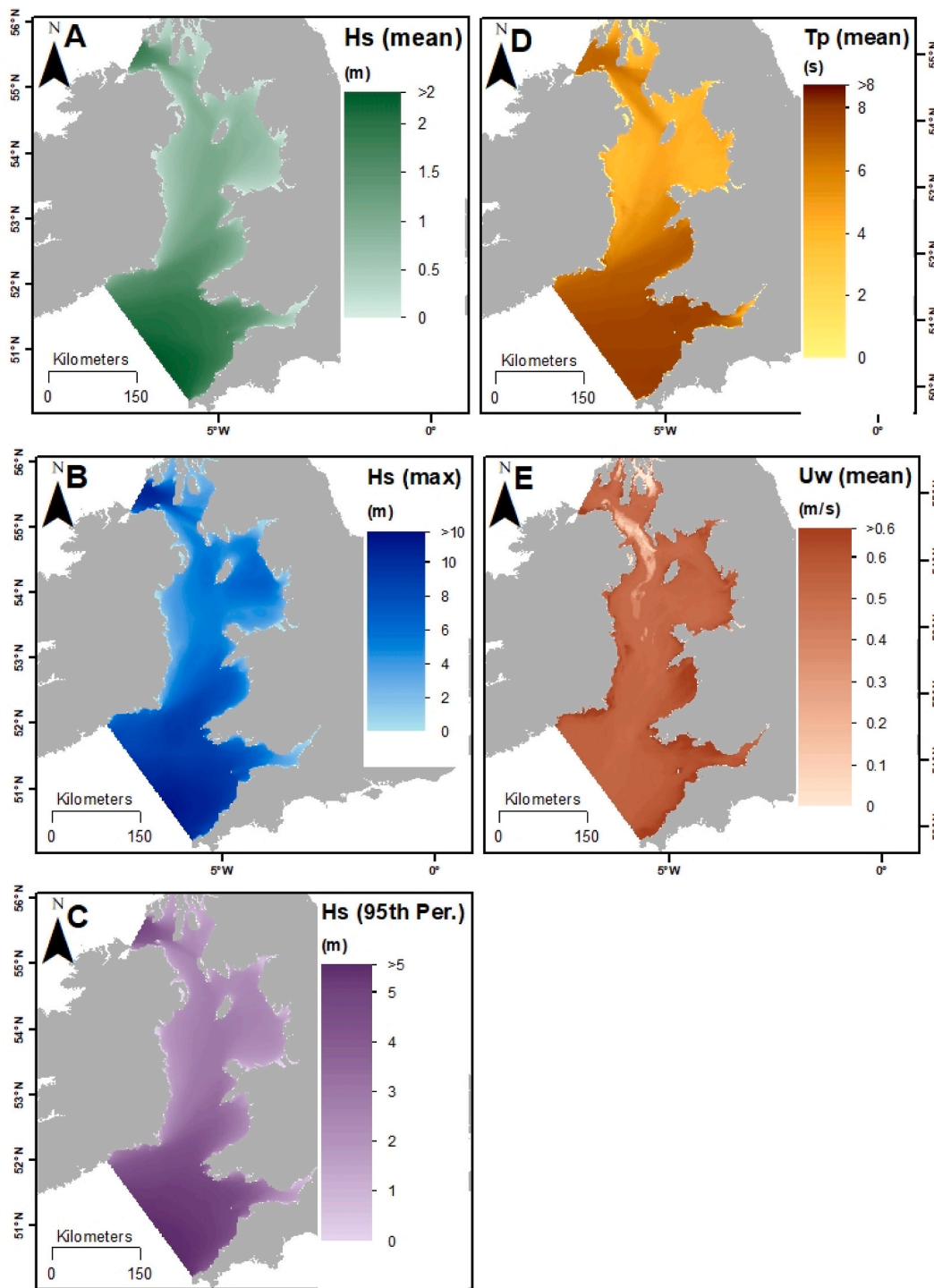


Fig. 7. Maps of simulated wave characteristic outputs. A: mean significant wave height (Hs) in metres. B: maximum significant wave height (Hs) in metres. C: 95th percentile of the significant wave height (Hs) in metres. D: mean wave period (Tp) in seconds. E: mean near-bed orbital velocity due to wave ( $U_w$ ) in metres per second (m/s).

Gallagher et al. (2014) broadly concur with those presented in Fig. 7B. Similarly, mean historical values for maximum Hs of up to 5 m in the central Irish Sea and 10 m in the Celtic Sea approaches reported by Tiron et al. (2015) also corroborate values presented in Fig. 7B. Whilst the difference between mean and maximum Hs is significant, the Hs 95<sup>th</sup> percentile value highlights the influence of extreme weather events on the maximum Hs value. Overall, values generated for the 95<sup>th</sup> percentile showed good agreement with those produced by Gleeson et al. (2017). In general, average wave conditions generate near-bed horizontal

orbital velocities ( $U_w$ ) in the Irish Sea that are low (less than 0.1 m/s; Fig. 7E), with stronger values confined to nearshore areas and along the Bristol Channel (Fig. 7E). These simulated wave values were used to calculate bed shear stress values due to wave ( $\tau_w$ ) according to Equation (8).

#### 4.3. Bed shear stress and sediment mobilisation

The annual mean value for bed stress induced by both wave and

current ( $\tau_{cw}$ ) in the Irish Sea is approximately  $0.5 \text{ N/m}^2$  (Fig. 8). Mean values are highest in the North Channel, Cardigan Bay, Caernarfon Bay and off the southeast coast of Ireland (Wexford/Waterford) (Fig. 8).

Mobilisation Frequency Index (MFI) values for  $\tau_c$  exceedance range from 0 to 98% (Fig. 9), with a spatial mean value of  $\sim 27\%$ . High levels of exceedance ( $>50\%$ ) are noted in the North Channel and in the Bristol Channel. Values for  $\tau_w$  exceedance range between 0 and 90% (Fig. 9), with a mean value of  $\sim 6\%$ . Areas which show greatest exceedance ( $>20\%$ ) are generally in shallower water depths of  $<20 \text{ m}$ . Combined current and wave induced bed shear stress ( $\tau_{cw}$ ) increases the mean exceedance to  $\sim 31\%$ .

By evaluating the percentage time of exceedance, or mobilisation frequency, a spatial assessment of the relative importance of each of these physical processes in mobilising sediment was carried out. In this scheme, for “tide” to be classified the dominant disturbance process of an area, the time percentage of mobilization by tidal currents (in that area) must be greater than twice that of by waves. Areas dominated by “wave” processes are similarly defined, and areas where no process meets these criteria are set as “mixed”. Most of the sediment mobilisation in the Irish Sea is calculated as tide dominated (Fig. 10A). Areas of wave-dominated sediment mobilisation are mainly close to shore ( $<20 \text{ km}$ ). Results from the SDI and SMI calculations are presented in Figs. 10B and C respectively. The SDI is scaled from 0 to 1.6 with the highest levels of disturbance ( $>0.5$ ) located in the North Channel, off the southeast coast of Ireland and around Caernarfon and Cardigan Bay. The mean disturbance is 0.01 and values are generally less than 0.1 throughout the Irish Sea. The SDI scheme can potentially be used as a means of comparing absolute sediment disturbance in various continental shelf regions (Li et al., 2015). Maximum SDI values of up to 1.6 found in this study are slightly lower than those for the Bay of Fundy of 1.7–2 calculated by Li et al. (2015). The mean value for the areas of highest sediment disturbance in the Australian shelf is approximately 1.3 (Hemer, 2006). Typically, the range of values for SMI in the Irish Sea is 0–3, although values  $>5$  have been calculated in this study. The lowest indexed areas (0–0.5) correspond with the mud patches West and east of the Isle of Man (the WISMB and EISMB respectively), as well as in the

Celtic Sea. With this range of values, the Irish Sea exhibits higher levels of sediment mobility in comparison to other studies for shallow continental shelf settings using the SMI. For the Bay of Fundy, Li et al. (2015) estimated an SMI from 0–2. Whilst for Sable Island Bank an SMI of up to 1.2 was found (Li et al., 2009). In a modelling study for the Canadian continental shelves the estimated range of SMI is from 0–2 and that the SMI values on the Australian Shelf should also be in the range of 0–2 based on the magnitude of SDI values reported in Hemer (2006), (Li et al., 2021). SMI values presented in this study are more comparable to reported SMI values ranging between 0 and 4.5 under normal tidal conditions for Galway Bay off the Irish West Coast in Joshi et al. (2017). Despite the high levels of mobilisation frequency in the Irish Sea (Fig. 9), the mean SMI value is 0.8 with the highest indexed areas ( $>3$ ) found in the North Channel, north of the Isle of Man and the Bristol Channel, where tidal currents are constricted and bed stresses increased, as well as embayments and along coastlines where wave action can play a more prominent role.

## 5. Discussion

A key outcome from this study is the spatial quantification of tidal current, wave and combined tide and wave induced stress on the Irish Sea seabed and the patterns of sediment mobilisation this induces. The combination of calibrated hydrodynamic and wave models with an extensive sediment properties database allows for a practical and flexible interrogation of seafloor sediment dynamics in terms of mobilisation frequency. Up to 35% of the sediment coverage spatially within study area (i.e. the Irish Sea and its approaches) is mobilised more than 50% of the time in the timeframe studied (i.e. 1 year). Only 2% of the study area was calculated as experiencing 0% sediment mobility. Results highlight that tidal current induced bed stress is the driving force of sediment mobility, with wave induced bed stress mainly acting on nearshore areas  $<10 \text{ km}$  from shore on the west coastline of the Irish Sea and  $<20 \text{ km}$  on the eastern coastline. The data generated allows for a more holistic understanding of the controlling physical processes behind sediment dynamics in the Irish Sea, which has implications for the

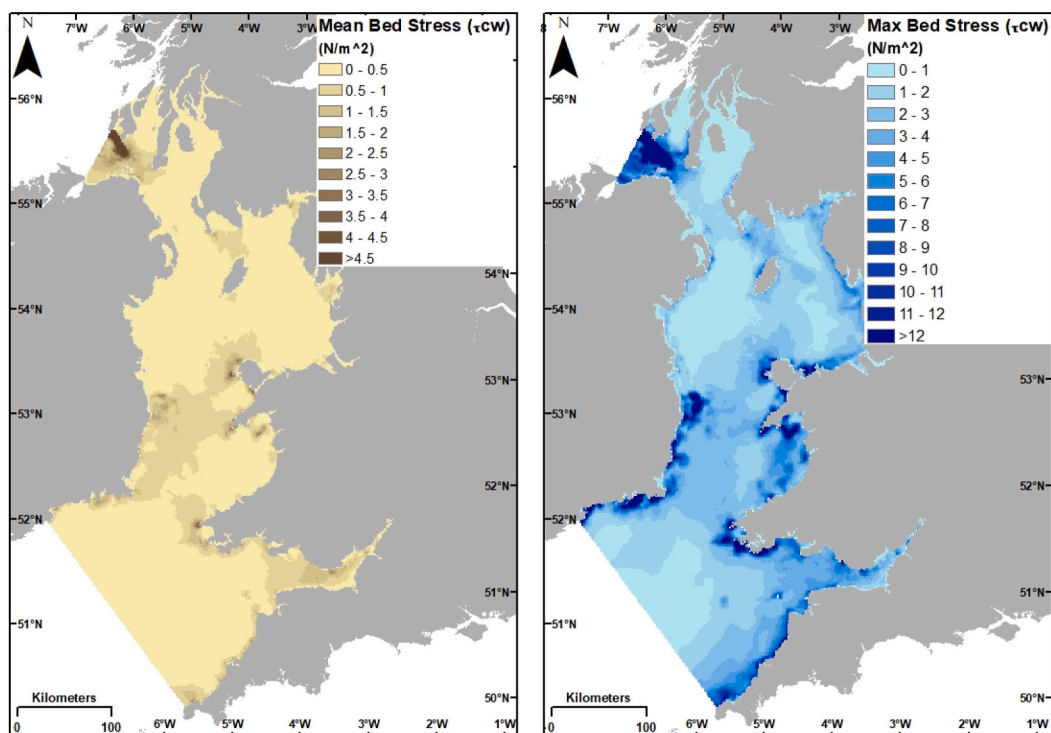


Fig. 8. Maps of bed shear stress for combined current and wave ( $\tau_{cw}$ ). Left panel displays mean  $\tau_{cw}$  values and the right panel displays maximum  $\tau_{cw}$  values.

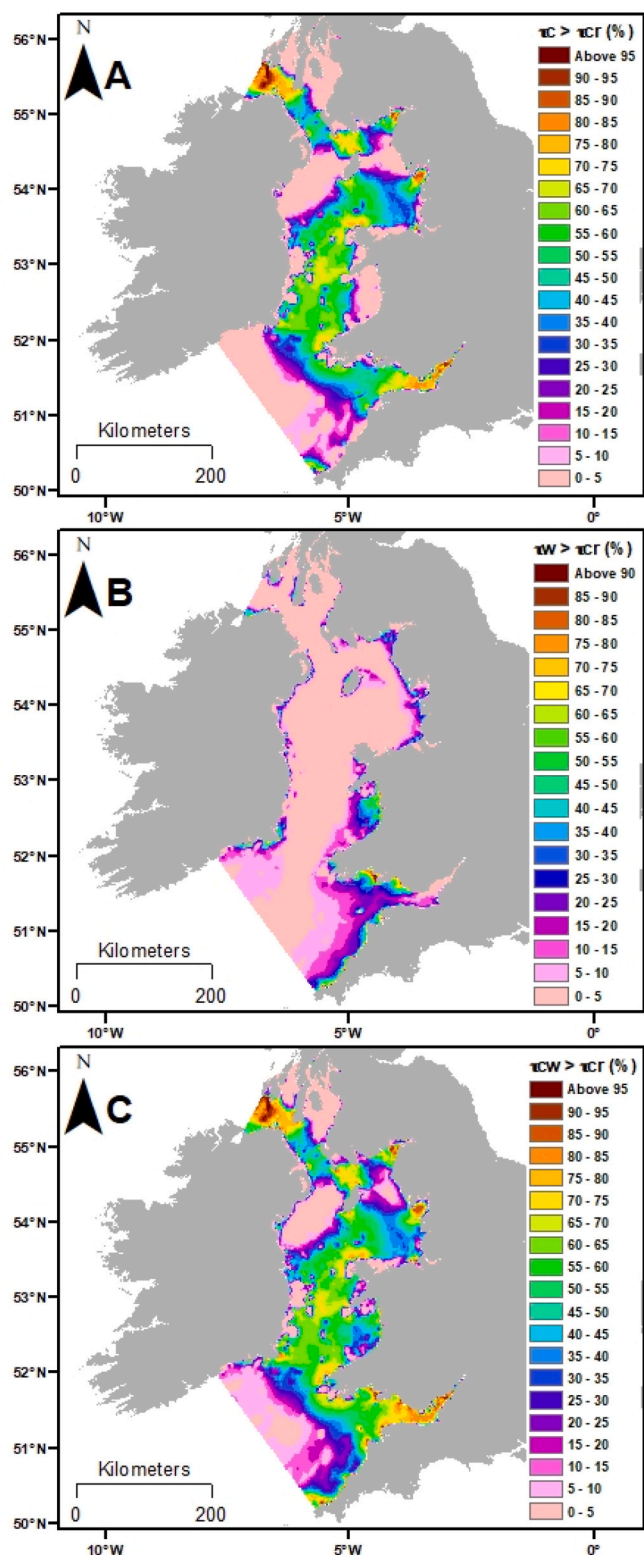


Fig. 9. Mobilisation Frequency Index (MFI) data showing yearly exceedance of A:  $\tau_c > \tau_{cr}$ , B:  $\tau_w > \tau_{cr}$  and C:  $\tau_{cw} > \tau_{cr}$ .

understanding of seabed geomorphology, the installation of offshore engineering structures and benthic habitats.

### 5.1. Model applications

Simulated current velocities were highest (up to 3 m/s) in the North

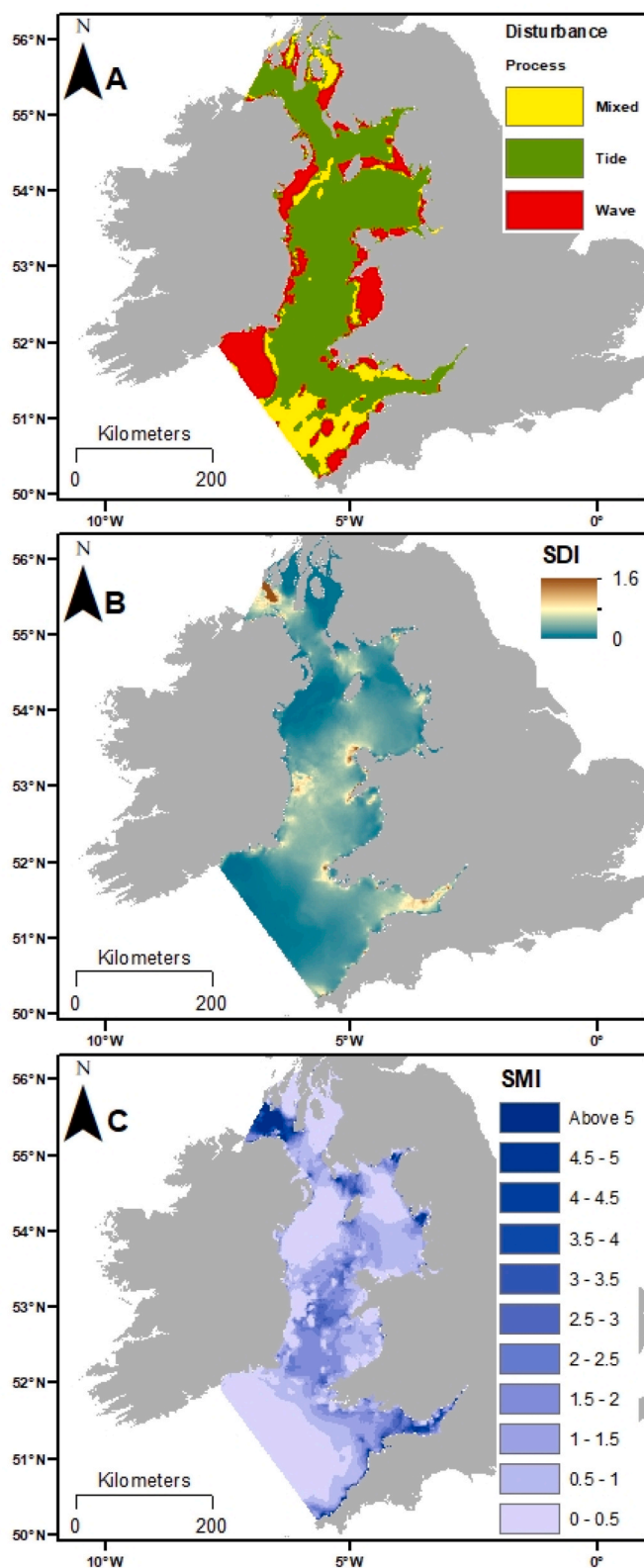


Fig. 10. Fig. 10 A: regional importance of seabed disturbance by different dominant processes, B: Sediment Disturbance Index (SDI) and C: Sediment Mobility Index (SMI).

Channel, where speeds of 1.8 m/s have been recorded previously (Knight and Howarth, 1999). Areas of strong currents are notable near headlands such as Carnsore Point in southern Ireland, Wicklow Head, northwest of Anglesey, the Llŷn Peninsula, offshore Pembrokeshire,

south of Mull of Galloway and north of Isle of Man (Fig. 6). Headlands commonly act as focal points for tidal energy with enhanced bed shear stress as a result (King et al., 2019). These areas have been identified as potential sites for tidal-stream renewable energy installations (Lewis et al., 2015; Robins et al., 2015). Considering sites for tidal energy converters typically require tidal current velocities in excess of 2.5 m/s, they are particularly susceptible to the mobilisation of sediment and especially the erosion of sediment causing seabed instability or ‘scour’ (Chen and Lam, 2014). Despite experiencing strong tidal current speeds, sediments in the areas of Wicklow Head, Anglesey, the Llŷn Peninsula, Pembrokeshire experience low mobilisation frequency of <5% (Fig. 9A). In these areas the sediments are coarse-grade sands and gravel patches with cobbles noted in places (Ward et al., 2015, Figs. 5B and 11). Regional seabed mapping by the BGS highlights rock and with thin sediment cover in the areas of Anglesey and the Llŷn Peninsula (Fig. 11). It is likely that the strong currents in these areas has mobilised finer sediment and transported it elsewhere. This winnowing, along with continued erosion, has exposed even coarser sediments resulting in a

more stable seabed in terms of sediment mobilisation. Additionally, the hidden exposure effect of grains in sediment mixtures can require significant increases in the bed shear stress required to mobilise certain sediment fractions (McCarron et al., 2019). In this regard, it is possible that these areas of high current speed, but low sediment mobilisation frequency, may be preferable for siting tidal energy converters as scour may not have such a significant impact.

Relatively high tidal current speeds (up to 2.2 m/s) occur in the central Irish Sea between Wicklow Head and the Llŷn Peninsula (Fig. 6). This area coincides with a degenerate amphidrome (an area where there the tidal range is nearly zero, but with strong tidal currents) which marks a bedload parting zone where there are divergent patterns in sediment transport direction (Holmes and Tappin, 2005; Van Landeghem et al., 2009) (Fig. 11). Mean tidal current values progressively weaken northward from this parting zone. Sediments in the vicinity of bedload parting zones consist of coarse-grained material of sand and gravel, as well as areas of diamicton to the south (Figs. 5B and 11). The sediments form a range of bedforms which are known to be dynamic

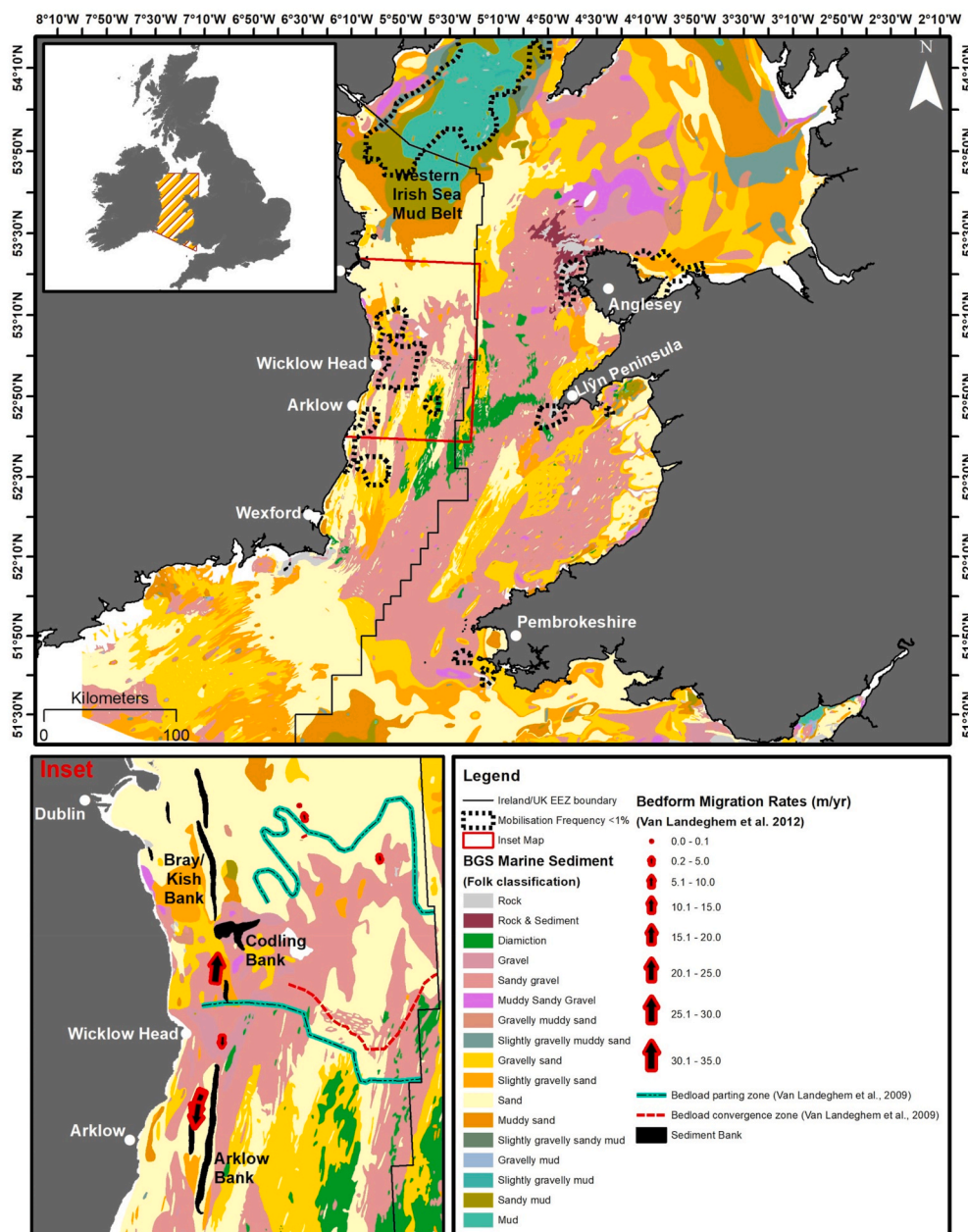


Fig. 11. Seabed substrate types in the Irish Sea according to BGS data. Highlighted in the main map are areas of low sediment mobilisation frequency (<1%). In the inset map sediment banks in the Irish Sea are noted in addition to sediment wave direction (Van Landeghem et al., 2009), bedload parting zones (Van Landeghem et al., 2009) and indicative, average bedform migration rates (Van Landeghem et al., 2012). Also highlighted are geographic locations and features mentioned in the text.

with average bedform migration rates up to 32 m/yr (Van Landeghem et al., 2012, Fig. 11). Migrating bedforms typically correspond with areas where the mobilisation frequency of sediments is 10% or more. However, bedforms with higher migration rates (32 m/yr) can occur in areas where the mobilisation frequency values are typically less than 10%, with some features with migration rates of up to 6 m/yr occurring in areas where sediment mobilisation frequency is less than 5% of the time. This highlights how considerable amounts of sediment movement can occur over long (interannual) time periods, even though mobilisation events occur infrequently. Another explanation could relate to the grain-size values used in the mobilisation frequency calculations. This study considers the mobilisation of sediment in terms of bed shear stress values exceeding sediment thresholds based on a median grain-size (i.e. D50) value. The sediments in the Irish Sea are typically reworked glacial deposits and so are generally poorly-sorted consisting of sand and sandy gravels (Fig. 11). Multi-modal sediments can have a fines component that may be mobilised by a bed shear stress value lower than the overall D50 value predicts (Griffin et al., 2008). Sediment waves in the Irish Sea are known to comprise of various sediment grades (Van Landeghem et al., 2009), often with fine-grained sediment veneers at the crest and coarse-grained flanks and troughs (Van Landeghem et al., 2009). It is therefore possible that the finer sediment component is mobilised more frequently resulting in changes in crest position and morphology with coarser sediments remaining more stable. In such areas of mixed sediment, estimating a median grain-size value that is representative is elusive (Ward et al., 2015). Whilst bathymetric variation as a result of seafloor bedforms can be captured by the model, it cannot account fully for the smaller scale spatial variability of bed roughness produced by such bedforms. Such variation can have a localised influence on critical bed shear stress and current energy dissipation (Kagan et al., 2012; Van Landeghem et al., 2012). The link between sediment mobility and bedform migration has important implications for the siting of offshore infrastructure as it can lead to significant changes in seabed levels causing the burial or exposure of structures such as cables or pipelines. (e.g. Drago et al., 2015). Further work in this area could develop more localised models for areas of sediment waves using higher resolution bathymetry and a greater density of granulometric analysis from sediment samples across bedform profiles to study hydrodynamic controls on sediment wave morphology and behaviour.

In addition to sediment waves, a series of well-documented, linear, north-south trending sandbanks are found close inshore and parallel to the Wexford, Wicklow and South Dublin coast (Fig. 11). These banks form a punctuated line of bathymetric highs parallel to the coast, which are often <5m below sea-level, with breaks between them maintained by strong currents and sediment movement. Many of these bedforms are considered as relics, formed under more energetic tidal regimes in the geological past (Uehara et al., 2006; Wheeler et al., 2001) or with a partly glacial origin (Whittington, 1977). The banks themselves are believed to be quasi-stable over historical time, in dynamic equilibrium with hydrographic conditions (Warren and Keary, 1988; Wheeler et al., 2001). Sediment banks are of considerable importance as they can offer coastal protection, areas for aggregate extraction and nurseries for fisheries (Dyer and Huntley, 1999). A number of these banks (including Arklow, Codling, Bray and Kish) are the focus of offshore windfarm development (Guinan et al., 2020). At present there are seven turbines erected at Arklow Bank since 2004, which experienced significant scour shortly after construction (Whitehouse et al., 2011). Understanding bank development and maintenance is difficult as morphology can evolve over long-term time intervals and observation may be episodic (e.g. interannual bathymetric surveys). Bank behaviour can be cyclical or part of a trend whereby changes might be episodic, as a result of high-magnitude low-frequency events like storms, or gradual as a result of tidal processes (Dolphin et al., 2007). As a combination of wave and tidal processes can influence bank morphological change, understanding both episodic and gradual changes on shorter term time scales than

interannual surveys can help determine what the dominant processes are driving bank dynamics (Whitehouse et al., 2011). Despite the shallow water depths, tide is still the dominant process controlling sediment disturbance at these sediment banks with the exception of wave for Codling Bank (Fig. 10A). However, sediment mobilisation frequency values for Codling bank for current and wave are both very low at <1% and <5% respectively. Sediment mobilisation frequency calculations exhibit high values based on  $\tau_{cw}$  for Arklow Bank (up to 67%), more moderate levels for Bray and Kish Banks (approximately 47%) and low levels for Codling Bank (typically <5%). Still, wave action can have an important role in mobilising sediment (e.g. up to 20% sediment mobilisation frequency for Arklow Bank) and would need to be considered as part of any scour analysis. Based on sediment mobilisation data, it would be expected that Arklow Bank is the most susceptible to morphological change and Codling Bank the least. The lower mobilisation frequency for Codling Bank can be explained by the fact that the seabed substrate in the area is coarser (sandy gravel to gravel) than at Arklow, Bray or Kish Bank (sand) resulting in a higher threshold for sediment mobilisation due to higher D50 values (Figs. 5B and 11). The notions that these sandbanks are relics and quasi-stable should be re-considered in light of the seabed shear stress and sediment mobility findings of the present study.

Mud patches are also present (Fig. 11), and often correspond to areas with low to negligible sediment mobilisation (Fig. 9C). Sediment MFI values of near 0% and SMI values of 0–0.5 are calculated for the areas of fine-grained sediment located to the west of the Isle of Man, referred to as the Western Irish Sea Mud Belt (WISMB), and to a lesser extent the Eastern Irish Sea Mud Belt (EISMB) on the opposing side of the Irish Sea. The low MFI and SMI values calculated are likely due to the low tidal current speeds and corresponding bed stress conditions experienced by these areas (Figs. 6 and 8). As a result, it has been demonstrated that this area is a zone of sediment deposition rather than erosion, and that sediment has been deposited there continuously over the Holocene period (Coughlan et al., 2015; Kershaw, 1986; Woods et al., 2019). The approach adopted here for calculating sediment mobility here (i.e. Whitehouse, 1998) is primarily valid for non-cohesive sediments. It is well recognised that predicting the dynamics of clay-rich or mud-grade sediment is difficult due to the cohesive potential (Ward et al., 2015; Williams et al., 2019). However, it is likely that the sediments in the WISMB are more silt dominated than clay-rich, and so the sediments are more non-cohesive than cohesive in nature (Coughlan et al., 2019). Despite the low levels of sediment mobilisation, the WISMB is subject to a seasonal hydrographic phenomena whereby surface heating of the water mass is sufficient to overcome tidal mixing generating density contrasts which drive a gyre effect (Horsburgh et al., 2000; Olbert et al., 2011). The geographic extent of this seasonal gyre corresponds with the area of low sediment mobilisation within the WISMB, and reported current speeds of <0.2 m/s in Horsburgh et al. (2000) are comparable with current speeds simulated here (Fig. 6). However, the gyre is reported to affect current flow at the seabed and enhance the erosion potential, particularly around seabed obstacles (Callaway et al., 2009). Again, this can have implications for infrastructure (e.g. turbine foundations, cables, pipelines) in this area in terms of stability. In order to fully resolve the baroclinic conditions that are fundamental to the development of seasonal thermal stratification that drives the gyre, a comprehensive 3D hydrodynamic model (with heat input included in the model forcing) would be required (e.g. Horsburgh et al., 2000).

A number of modelling studies have demonstrated that storm-induced currents and background ocean currents are important in affecting bed shear stress and sediment mobilization on some areas of the continental shelves (Harris et al., 2000; Hemer, 2006; Porter-Smith et al., 2004). Whilst the occurrence of storm surge and associated currents may impact locally on the hydrodynamic regime and, therefore, in turn the sediment mobilization, these storms are typically short-lived with respect to the timeframe simulated and their effect is mostly of importance in shallower water, typically <20 m (Fig. 9B; Ward et al.,

2020). It can be expected that, at present, averaged over the year the sediment mobilization patterns will not be significantly impacted by occurrence of storms.

## 5.2. Environmental implications

Trawling using bottom fishing gear has been shown as an anthropogenic activity which can cause significant seabed sediment disturbance and remobilisation (e.g. O'Neill and Summerbell, 2011; Palanques et al., 2001). Trawling intensity is most heavily concentrated in the WISMB for the Dublin Bay Prawn (*Nephrops norvegicus*) (Kaiser et al., 1996; O'Higgins et al., 2019). Whilst sediment mobilisation levels for the WISMB have been calculated to be naturally low, trawling has been shown to have a high impact on sediment disturbance with loss of seabed, sediment coarsening and weakening of sediment shear strength recorded (Coughlan et al., 2015). Given the low levels of sediment mobility in the WISMB, this sediment coarsening is likely to persist. This could have implications on the habitat and ecological success of the *Nephrops*, which prefer sediment with moderately high silt-clay ratios (i.e. low sand) for burrow construction (Johnson et al., 2013). Given that the WISMB accounts for 25% of the total Irish Sea seabed trawled from April to December, with up to 55% fishing intensity (Kaiser et al., 1996) further work is required in order to understand the implications of trawling induced sediment mobilisation in this area. This is also true for areas where sediment is more frequently mobilised which are also trawled as induced remobilisation of sediment could similarly alter the habitats of the species being trawled.

Whilst there is currently no database of microplastics in Irish Sea sediments, studies have found high levels of microplastic ingested by *Nephrops norvegicus* in the WISMB (Hara et al., 2020). Often microplastics are found shallower than 2.5 cm below the seafloor, with substantial proportions in the upper 0.5 cm (Martin et al., 2017). Many microplastics examined have been linked to fishing gear, and their disintegration can be a consequence of physical forces and abrasion due to sediment transport (Martin et al., 2017). Given the significant amount of trawling that occurs in the WISMB, and the low-levels of sediment disturbance, it is possible that the WISMB could act as a long-term repository for microplastic accumulation, which could have implications for exposure and risk of human consumption. Models for the transport, deposition and accumulation of microplastics remain understudied, but they are known to reside in seafloor sediments and are so intrinsically linked with sediment mobilisation and transport (Kane and Clare, 2019).

On the eastern side of the Irish Sea, the Sellafield nuclear complex (located in Cumbria, west coast of the UK) has been discharging low-level waste into the area offshore since 1951 (Gray et al., 1995). This area, the EISMB, is an important source of contaminant radionuclides, including  $^{137}\text{Cs}$ ,  $^{241}\text{Am}$  and Pu, which have been incorporated into the sediments there (MacKenzie et al., 1999). These anthropogenic radionuclides were initially restricted to the area extending approximately 5 km offshore from the point of discharge and, although overall levels of output from Sellafield into the Irish Sea have decreased steadily since the 1980s, radionuclides like  $^{241}\text{Pu}$  and  $^{241}\text{Am}$  have long-term availability due their half-lives (e.g. 14 years for Pu) (Ray et al., 2020). Other radionuclides (i.e.  $^{99}\text{Tc}$ ) have a low accumulation rate in sediment, but are known to have a long half-life and are transported by water circulation patterns to the east coast of Ireland (Olbert et al., 2010). Whilst concentrated in the EISMB, minimums in radionuclide concentrations are observed in areas of coarse sediments and high sediment dispersion due to strong currents, such as north of the Isle of Man and the North Channel (MacKenzie et al., 1999). Furthermore, radionuclide-contaminated particles are typically transported in the clay and silt range of sediment and instances of accumulation have been well-documented in cores from the WISMB (Coughlan et al., 2015; Kershaw et al., 1990; Mitchell et al., 1999). Therefore, remobilisation and suspension of sediment is a key process in the dispersion of radionuclides bound to sediment particles and understanding presently active

sediment mobilisation and sedimentation processes is critical to accurately predicting the re-distribution and fate of sediment-bound contaminants (Hunt and Kershaw, 1990; Kershaw et al., 1999; MacKenzie et al., 1999). Sediment MFI levels for the area offshore Sellafield range up to 30%, with a notable wave component (Fig. 9). This frequency of mobilisation is likely to have a significance influence in the mobilisation of radionuclide-contaminated sediment, which is particularly concentrated in finer sediments, and preventing it from being buried by the low levels of sedimentation in the EISMB (Kershaw et al., 1988). Therefore, surface sediments are likely to remain a source of radionuclides to be transported elsewhere in the Irish Sea by hydrodynamic processes and so effective monitoring is required (e.g. Olbert et al. (2010).

Seabed morphology, sediment type and bed shear stress are key parameters used in habitat mapping and prediction (Kostylev et al., 2001; Todd and Kostylev, 2011). The highly variable substrate and geomorphology of the Irish Sea means it contains a diverse range of habitat settings (e.g. Robinson et al. (2011)). The use of static substrate maps severely hampers the ability to predict changes in biological environment and species diversity due to sediment mobilisation. Callaway et al. (2009) showed how sediment removal (i.e. scour) even in a low-energy environment in the Irish Sea can affect community composition. Therefore, incorporating seabed disturbance and sediment mobility into seabed habitat mapping becomes important for predicting spatial and temporal changes (Kostylev and Hannah, 2007; Porter-Smith et al., 2004). In this regard, the MFI, SDI and SMI data presented in this study (Figs. 9 and 10B&C) can be used in combination with biological and other physical data to identify habitats or species potentially at risk as a result of sediment mobilisation from short to long-term timeframes (Huang et al., 2011).

## 6. Conclusions

The frequency of mobility of sediments in the Irish Sea has been calculated for the first time using a calibrated, regional-scale hydrodynamic and wave models and an extensive grab sample database. Sediment mobilisation frequency by tidal current, wave and combined tidal current and wave induced bed stress was calculated based on the threshold exceedance of the Shields criterion. A Sediment Disturbance Index (SDI) and a Sediment Mobility Index (SMI) were calculated to characterise the magnitude in addition to the frequency of seabed exposure and threshold exceedance respectively. Sediment mobility is prevalent across the Irish Sea with only 2% calculated as experiencing 0% sediment mobility. The spatial quantification of sediment mobility calculated in this study has greatly improved our knowledge and understanding of sediment dynamics in the Irish Sea in terms of identifying areas where seabed mobility is low and so where sites are likely to be stable for the deployment of offshore infrastructure like wind turbines. Conversely, indices calculated have identified areas where sediment mobility is high and so potential areas where benthic habitats may already be under significant natural disturbances. As a result, the indices calculated are useful tools for marine spatial planning and for devising seabed management strategies.

### Model bounding coordinates

7.63° W, 56.3° N  
1.77° W, 56.14° N  
2.56° W, 50.05° N  
7.68° W, 50.19° N

### Data availability

The bathymetric metadata and Digital Terrain Model data products have been derived from the EMODnet Bathymetry portal - <http://www.emodnet-bathymetry.eu>. This paper contains Irish Public Sector Data (INFOMAR) licensed under a Creative Commons Attribution 4.0

International (CC BY 4.0) licence and accessed through <https://www.infomar.ie>. The digital seabed sediment map (DigSBS250) was made available by the BGS through <https://www.bgs.ac.uk/datasets/marine-sediments-250k/>. Tide gauge data are available from The UK National Tide Gauge Network, provided by the British Oceanographic Data Centre, and the Marine Institute accessed through <https://www.digitalocean.ie/>. Wave buoy data are available from Met Éireann and accessed at [www.met.ie](http://www.met.ie). This study uses ERA5 dataset available from Copernicus Climate Change Service (C3S) through the ECMWF website <https://www.ecmwf.int/en/forecasts/datasets/reanalysis-datasets/era5>.

### Declaration of competing interest

The authors declare that they have no known competing financial interests or personal relationships that could have appeared to influence the work reported in this paper.

### Acknowledgements

This project (Grant-Aid Agreement No. IND/18/18) is carried out with the support of the Marine Institute under the Marine Research Programme 2014–2020, co-financed under the European Regional Development Fund, with the work undertaken through a close industry-academic collaboration involving Gavin and Doherty Solutions (GDG - engineering consultancy), University College Dublin (iCRAG) and University College Cork (MaREI). MC is funded under an Irish Research Council Enterprise Partnership Scheme Postdoctoral Fellowship (EPSPD/2020/109) and in part by a research grant from Science Foundation Ireland (SFI) under Grant Number 13/RC/2092, with support from Gavin and Doherty Geosolutions Ltd and the Geological Survey of Ireland (GSI). SC is funded under an Irish Research Council Employment-Based Postgraduate Programme Scholarship (EBPPG/2019/158). The authors are grateful for access to the seabed sediment sample data and would like to acknowledge colleagues collecting and preparing these data through the projects and surveys mentioned. The authors wish to thank Xavi Monteys and Charise McKeon (both GSI) in particular for aiding with the INFOMAR dataset. We would also like to thank Dave Hardy (GSI) for assistance with formatting bathymetry data. The authors would like to express gratitude to two anonymous reviewers who provided very valuable feedback that greatly improved the manuscript.

### References

- Belderson, R.H., 1964. Holocene sedimentation in the western half of the Irish Sea. *Mar. Geol.* 2, 147–163.
- Bever, A.J., MacWilliams, M.L., 2013. Simulating sediment transport processes in San Pablo Bay using coupled hydrodynamic, wave, and sediment transport models. *Mar. Geol.* 345, 235–253. <https://doi.org/10.1016/j.margeo.2013.06.012>.
- Bidlot, J., Janssen, P., Abdalla, S., Hersbach, H., 2007. A Revised Formulation of Ocean Wave Dissipation and its Model Impact. ECMWF, Reading, UK. <https://doi.org/10.21957/m97gmhqe>.
- Blott, S.J., Pye, K., 2001. GRADISTAT: a grain size distribution and statistics package for the analysis of unconsolidated sediments. *Earth Surf. Process. Landforms* 26, 1237–1248.
- Bolam, S.G., Barrio-Frojan, C.R.S., Eggleton, J.D., 2010. Macrofaunal production along the UK continental shelf. *J. Sea Res.* 64, 166–179. <https://doi.org/10.1016/j.seares.2010.02.003>.
- Bowden, K.F., 1980. Physical and dynamical oceanography of the Irish sea. In: Banner, F. T., Collins, M.B., Massie, K.S. (Eds.), *The North-West European Shelf Seas: The Sea Bed and the Sea in Motion II. Physical and Chemical Oceanography, and Physical Resources*. Elsevier, pp. 391–413.
- Callaway, A., Smyth, J., Brown, C.J., Quinn, R., Service, M., Long, D., 2009. The impact of scour processes on a smothered reef system in the Irish Sea. *Estuar. Coast Shelf Sci.* 84, 409–418. <https://doi.org/10.1016/j.eccs.2009.07.011>.
- Chen, L., Lam, W.H., 2014. Methods for predicting seabed scour around marine current turbine. *Renew. Sustain. Energy Rev.* 29, 683–692. <https://doi.org/10.1016/j.rser.2013.08.105>.
- Constantin, P., Foias, C., 1988. *Navier-Stokes Equations*. The University of Chicago Press, Chicago, London. <https://doi.org/10.1007/BF00047090>.
- Cooper, K.M., Curtis, M., Wan Hussin, W.M.R., Barrio Froján, C.R.S., Defew, E.C., Nye, V., Paterson, D.M., 2011. Implications of dredging induced changes in sediment particle size composition for the structure and function of marine benthic macrofaunal communities. *Mar. Pollut. Bull.* 62, 2087–2094. <https://doi.org/10.1016/j.marpolbul.2011.07.021>.
- Coughlan, M., Long, M., Doherty, P., 2020. Geological and geotechnical constraints in the Irish Sea for offshore renewable energy. *J. Maps* 16, 420–431. <https://doi.org/10.1080/17445647.2020.1758811>.
- Coughlan, M., Wheeler, A.J., Dorschel, B., Long, M., Doherty, P., Mörz, T., 2019. Stratigraphic model of the Quaternary sediments of the Western Irish Sea Mud Belt from core, geotechnical and acoustic data. *Geo Mar. Lett.* 39, 223–237.
- Coughlan, M., Wheeler, A.J., Dorschel, B., Lordan, C., Boer, W., Van Gaever, P., de Haas, H., Mörz, T., 2015. Record of anthropogenic impact on the Western Irish Sea mud belt. *Anthropocene* 9, 56–69. <https://doi.org/10.1016/j.ancene.2015.06.001>.
- Dalyander, P.S., Butman, B., Sherwood, C.R., Signell, R.P., Wilkin, J.L., 2013. Characterizing wave- and current- induced bottom shear stress: U.S. middle Atlantic continental shelf. *Contin. Shelf Res.* 52, 73–86. <https://doi.org/10.1016/j.csr.2012.10.012>.
- Department of Communications Climate Action and Environment DCCAE, 2019. *Climate Action Plan: to tackle climate breakdown*. Dublin. <https://doi.org/10.5860/CHOICE.46-0890>.
- DHI Group, 2019. MIKE 21 Toolbox: User Guide.
- DHI Group, 2017a. MIKE 21 & MIKE 3 Flow Model FM: Hydrodynamic and Transport Module.
- DHI Group, 2017b. Non-Cohesive Sediment Transport Module - Mike 21 ST.
- DHI Group, 2017c. MIKE 21 Flow Model - Hydrodynamic Module.
- DHI Group, 2017d. MIKE 21 Spectral Waves Module.
- Dobson, M.R., Evans, W.E., James, K.H., 1971. The sediment on the floor of the southern Irish Sea. *Mar. Geol.* 11, 27–69.
- Dolphin, T.J., Vincent, C.E., Coughlan, C., Rees, J.M., 2007. Variability in sandbank behaviour at decadal and annual time-scales and implications for adjacent beaches. *J. Coast Res.* 731–737.
- Drago, M., Mattioli, M., Bruschi, R., Vitali, L., 2015. Insights on the design of free-spanning pipelines. *Philos. Trans. R. Soc. A Math. Phys. Eng. Sci.* 373, 20140111. <https://doi.org/10.1098/rsta.2014.0111>.
- Dyer, K.R., Huntley, D.A., 1999. The origin, classification and modelling of sand banks and ridges. *Contin. Shelf Res.* [https://doi.org/10.1016/S0278-4343\(99\)00028-X](https://doi.org/10.1016/S0278-4343(99)00028-X).
- EMODnet Bathymetry Consortium, 2018. *EMODnet Digital Bathymetry (DTM 2018)*.
- Folk, R.L., 1954. The distinction between grain size and mineral composition in sedimentary-rock nomenclature. *J. Geol.* 62, 344–359.
- Folk, R.L., Ward, W.C., 1957. Brazos River Bar: a study in the significance of grain size parameters. *J. Sediment. Petrol.* 27, 3–26.
- Gallagher, S., Tiron, R., Dias, F., 2014. A long-term nearshore wave hindcast for Ireland: Atlantic and Irish Sea coasts (1979–2012). *Ocean Dynam.* 64, 1163–1180. <https://doi.org/10.1007/s10236-014-0728-3>.
- Gleeson, E., Gallagher, S., Clancy, C., Dias, F., 2017. NAO and extreme ocean states in the Northeast Atlantic Ocean. *Adv. Sci. Res.* 14, 23–33. <https://doi.org/10.5194/asr-14-23-2017>.
- Glock, K., Tritthart, M., Habersack, H., Hauer, C., 2019. Comparison of hydrodynamics simulated by 1D, 2D and 3D models focusing on bed shear stresses. *Water*. <https://doi.org/10.3390/w11020226>.
- Gray, J., Jones, S.R., Smith, A.D., 1995. Discharges to the environment from the Sellafeld site, 1951–1992. *J. Radiol. Prot.* 15, 99.
- Griffin, J.D., Hemer, M.A., Jones, B.G., 2008. Mobility of sediment grain size distributions on a wave dominated continental shelf, southeastern Australia. *Mar. Geol.* 252, 13–23. <https://doi.org/10.1016/j.margeo.2008.03.005>.
- Guinan, J., McKeon, C., O’Keeffe, E., Monteys, X., Sacchetti, F., Coughlan, M., Nic Aonghusa, C., 2020. INFOMAR data supports offshore energy development and marine spatial planning in the Irish offshore via the EMODnet Geology portal. *Q. J. Eng. Geol. Hydrogeol.* 54. <https://doi.org/10.1144/qjgeh2020-033>.
- Hara, J., Frias, J., Nash, R., 2020. Quantification of microplastic ingestion by the decapod crustacean *Nephrops nebulosus* from Irish waters. *Mar. Pollut. Bull.* 152, 110905. <https://doi.org/10.1016/j.marpolbul.2020.110905>.
- Harris, P.T., Smith, R., Anderson, O., Coleman, R., Greenslade, D., 2000. *GEOMAT - Modelling of Continental Shelf Sediment Mobility in Support of Australia’s Regional Marine Planning Process*, AGSO Record 2000/41.
- Hemer, M.A., 2006. The magnitude and frequency of combined flow bed shear stress as a measure of exposure on the Australian continental shelf. *Contin. Shelf Res.* 26, 1258–1280. <https://doi.org/10.1016/j.csr.2006.03.011>.
- Hill, A.E., Brown, J., Fernand, L., 1997. The summer gyre in the Western Irish Sea: shelf sea paradigms and management implications. *Estuar. Coast Shelf Sci.* 44, 83–95. [https://doi.org/10.1016/S0272-7714\(97\)80010-8](https://doi.org/10.1016/S0272-7714(97)80010-8).
- Hill, A.E., Durazo, R., Smeed, D.A., 1994. Observations of a cyclonic gyre in the western Irish Sea. *Contin. Shelf Res.* 14, 479–490.
- Holmes, R., Tappin, D.R., 2005. *DTI Strategic Environmental Assessment Area 6, Irish Sea, Seabed and Surficial Geology and Processes*, British Geological Survey Commissioned Report, CR/05/057.
- Holthuijsen, L.H., Herman, A., Booij, N., 2003. Phase-decoupled refraction-diffraction for spectral wave models. *Coast. Eng.* 49, 291–305.
- Horsburgh, K.J., Hill, A.E., Brown, J., Fernand, L., Garvine, R.W., Angelico, M.M.P., 2000. Seasonal evolution of the cold pool gyre in the western Irish Sea. *Prog. Oceanogr.* 46, 1–58. [https://doi.org/10.1016/S0079-6611\(99\)00054-3](https://doi.org/10.1016/S0079-6611(99)00054-3).
- Huang, Z., Brooke, B.P., Harris, P.T., 2011. A new approach to mapping marine benthic habitats using physical environmental data. *Contin. Shelf Res.* 31, S4–S16. <https://doi.org/10.1016/j.csr.2010.03.012>.



- Hunt, G.J., Kershaw, P.J., 1990. Remobilisation of artificial radionuclides from the sediment of the Irish Sea. *J. Radiol. Prot.* 10, 147–151.
- Idier, D., Romieu, E., Pedreros, R., Oliveros, C., 2010. A simple method to analyse non-cohesive sediment mobility in coastal environment. *Continent. Shelf Res.* 30, 365–377. <https://doi.org/10.1016/j.csr.2009.12.006>.
- Jackson, D.I., Jackson, A.A., Evans, D., Wingfield, R.T.R., Barnes, R.P., Arthur, M.J., 1995. United Kingdom Offshore Regional Report: the Geology of the Irish Sea. British Geological Survey, London.
- Johnson, H.K., Kofoed-Hansen, H., 2000. Influence of bottom friction on sea surface roughness and its impact on shallow water wind wave modeling. *J. Phys. Oceanogr.* 30, 1743–1756. [https://doi.org/10.1175/1520-0485\(2000\)030<1743:IOBPOS>2.0.CO;2](https://doi.org/10.1175/1520-0485(2000)030<1743:IOBPOS>2.0.CO;2).
- Johnson, M.P., Lordan, C., Power, A.M., 2013. Chapter two - habitat and ecology of Nephrops norvegicus. In: Johnson, M.L., Johnson, M.P.B.T.-A., M, B. (Eds.), *The Ecology and Biology of*. Academic Press, pp. 27–63. <https://doi.org/10.1016/B978-0-12-410466-2.00002-9>.
- Joshi, S., Duffy, G.P., Brown, C., 2017. Mobility of maerl-siliclastic mixtures: impact of waves, currents and storm events. *Estuar. Coast Shelf Sci.* 189, 173–188. <https://doi.org/10.1016/j.ecss.2017.03.018>.
- Kagan, B.A., Sofina, E.V., Rashidi, E., 2012. The impact of the spatial variability in bottom roughness on tidal dynamics and energetics, a case study: the M2 surface tide in the North European Basin. *Ocean Dynam.* 62, 1425–1442. <https://doi.org/10.1007/s10236-012-0571-3>.
- Kaiser, M.J., Hill, A.S., Ramsay, K., Spencer, B.E., Brand, A.R., Veale, L.O., K, P., Rees, E. I.S., Munday, B.W., Ball, B., Hawkins, S.J., 1996. Benthic disturbance by fishing gear in the Irish Sea: comparison of beam trawling and scallop dredging. *Aquat. Conserv. Mar. Freshw. Ecosyst.* 6, 269–285.
- Kane, I.A., Clare, M.A., 2019. Dispersion, accumulation, and the ultimate fate of microplastics in deep-marine environments: a review and future directions. *Front. Earth Sci.*
- Kershaw, P.J., 1986. Radiocarbon dating of Irish Sea sediments. *Estuar. Coast Shelf Sci.* 23, 295–303. [https://doi.org/10.1016/0272-7714\(86\)90029-6](https://doi.org/10.1016/0272-7714(86)90029-6).
- Kershaw, P.J., Denoon, D.C., Woodhead, D.S., 1999. Observations on the redistribution of plutonium and americium in the Irish Sea sediments, 1978 to 1996: concentrations and inventories. *J. Environ. Radioact.* 44, 191–221. [https://doi.org/10.1016/S0265-931X\(98\)00134-9](https://doi.org/10.1016/S0265-931X(98)00134-9).
- Kershaw, P.J., Swift, D.J., Denoon, D.C., 1988. Evidence of recent sedimentation in the eastern Irish Sea. *Mar. Geol.* 85, 1–14. [https://doi.org/10.1016/0025-3227\(88\)90081-3](https://doi.org/10.1016/0025-3227(88)90081-3).
- Kershaw, P.J., Woodhead, D.S., Malcolm, S.J., Allington, D.J., Lovett, M.B., 1990. A sediment history of Sellafield discharges. *J. Environ. Radioact.* 12, 201–241.
- King, E.V., Conley, D.C., Masselink, G., Leonardi, N., McCarroll, R.J., Scott, T., 2019. The impact of waves and tides on residual sand transport on a sediment-poor, energetic, and macrotidal continental shelf. *J. Geophys. Res. Ocean.* 124, 4974–5002. <https://doi.org/10.1029/2018JC014861>.
- Knight, P.J., Howarth, M.J., 1999. The flow through the north channel of the Irish Sea. *Continent. Shelf Res.* 19, 693–716. [https://doi.org/10.1016/S0278-4343\(98\)00110-1](https://doi.org/10.1016/S0278-4343(98)00110-1).
- Komen, G.J., Cavaleri, L., Donelan, M., Hasselmann, K., Hasselmann, S., Janssen, P., 1996. *Dynamics and Modelling of Ocean Waves*. Cambridge University Press, Cambridge, UK.
- Kostylev, V., Hannah, C., 2007. Process-driven characterization and mapping of seabed habitats. In: *Mapping the Seafloor for Habitat Characterization*. Geological Association of Canada, pp. 171–184.
- Kostylev, V.E., Todd, B.J., Fader, G.B.J., Courtney, R.C., Cameron, G.D.M., 2001. Benthic habitat mapping on the Scotian Shelf based on multibeam bathymetry, surficial geology and sea floor photographs. *Mar. Ecol. Prog. Ser.* 219, 121–137.
- Lewis, M., Neill, S.P., Robins, P.E., Hashemi, M.R., 2015. Resource assessment for future generations of tidal-stream energy arrays. *Energy* 83, 403–415. <https://doi.org/10.1016/j.energy.2015.02.038>.
- Li, M.Z., Hannah, C.G., Perrie, W.A., Tang, C.C.L., Prescott, R.H., Greenberg, D.A., 2015. Modelling seabed shear stress, sediment mobility, and sediment transport in the Bay of Fundy. *Can. J. Earth Sci.* 52, 757–775. <https://doi.org/10.1139/cjes-2014-0211>.
- Li, M.Z., Wu, Y., Hannah, C.G., Perrie, W.A., 2021. Seabed disturbance and sediment mobility due to tidal current and waves on the continental shelves of Canada. *Can. J. Earth Sci.* <https://doi.org/10.1139/cjes-2020-0139>. In press.
- Li, M.Z., Zou, Q., Hannah, C., Perrie, W., Prescott, R., Toulany, B., 2009. Numerical Modelling of Seabed Disturbance and Sediment Mobility with applications to Morphodynamics on the Storm-dominated Sable Island Bank, Scotian Shelf. GSC Open File 6155. <https://cdsciencepub.com/doi/pdf/10.1139/cjes-2020-0139>.
- MacKenzie, A.B., Cook, G.T., McDonald, P., 1999. Radionuclide distributions and particle size associations in Irish Sea surface sediments: implications for actinide dispersion. *J. Environ. Radioact.* 44, 275–296. [https://doi.org/10.1016/S0265-931X\(98\)00137-4](https://doi.org/10.1016/S0265-931X(98)00137-4).
- Manning, R., Griffith, J.P., Pigot, T.F., Vernon-Harcourt, L.F., 1890. *On the Flow of Water in Open Channels and Pipes*.
- Martin, J., Lusher, A., Thompson, R.C., Morley, A., 2017. The deposition and accumulation of microplastics in marine sediments and bottom water from the Irish continental shelf. *Sci. Rep.* 7, 1–9. <https://doi.org/10.1038/s41598-017-11079-2>.
- Martin, J., Puig, P., Palanques, A., Giamportone, A., 2015. Commercial bottom trawling as a driver of sediment dynamics and deep seascape evolution in the Anthropocene. *Anthropocene* 7, 1–15. <https://doi.org/10.1016/j.ancene.2015.01.002>.
- McCarron, C.J., Van Landeghem, K.J.J., Baas, J.H., Amoudry, L.O., Malarkey, J., 2019. The hiding-exposure effect revisited: a method to calculate the mobility of bimodal sediment mixtures. *Mar. Geol.* 410, 22–31. <https://doi.org/10.1016/j.margeo.2018.12.001>.
- Mellet, C., Long, D., Carter, G., Chiverrell, R., Van Landeghem, K., 2015. *Geology of the Seabed and Shallow Subsurface: The Irish Sea*. British Geological Survey Commissioned Report, CR/15/057, p. 52.
- Mitchell, P.I., Condren, O.M., Leo, L., McMahon, C.A., 1999. Trends in plutonium, americium and radiocaesium accumulation and long-term bioavailability in the western Irish Sea mud basin. *J. Environ. Radioact.* 44, 223–251.
- Nikuradze, J., 1933. *Strömungsgesetze in Rauhen Rohren*. VDI-Verlag.
- O'Higgins, T., O'Higgins, L., O'Hagan, A.M., Ansong, J.O., 2019. Challenges and opportunities for ecosystem-based management and marine spatial planning in the Irish sea. In: Zaucha, J., Gee, K. (Eds.), *Maritime Spatial Planning*. Springer International Publishing, Cham, pp. 47–69. [https://doi.org/10.1007/978-3-319-98696-8\\_3](https://doi.org/10.1007/978-3-319-98696-8_3).
- O'Neill, F.G., Summerbell, K., 2011. The mobilisation of sediment by demersal otter trawls. *Mar. Pollut. Bull.* 62, 1088–1097. <https://doi.org/10.1016/j.marpolbul.2011.01.038>.
- Olbert, A.I., Dabrowski, T., Nash, S., Hartnett, M., 2012. Regional modelling of the 21st century climate changes in the Irish Sea. *Continent. Shelf Res.* 41, 48–60. <https://doi.org/10.1016/j.csr.2012.04.003>.
- Olbert, A.I., Hartnett, M., 2010. Storms and surges in Irish coastal waters. *Ocean Model.* 34, 50–62. <https://doi.org/10.1016/j.ocemod.2010.04.004>.
- Olbert, A.I., Hartnett, M., Dabrowski, T., 2010. Assessment of Tc-99 monitoring within the western Irish Sea using a numerical model. *Sci. Total Environ.* 408, 3671–3682. <https://doi.org/10.1016/j.scitotenv.2010.04.053>.
- Olbert, A.I., Hartnett, M., Dabrowski, T., Mikolajewicz, U., 2011. Long-term inter-annual variability of a cyclonic gyre in the western Irish Sea. *Continent. Shelf Res.* 31, 1343–1356. <https://doi.org/10.1016/j.csr.2011.05.010>.
- Palanques, A., Guille, J., Puig, P., 2001. Impact of bottom trawling on water turbidity and muddy sediment of an unfished continental shelf. *Limnol. Oceanogr.* 46, 1100–1110.
- Peters, J.L., Butschek, F., O'Connell, R., Cummins, V., Murphy, J., Wheeler, A.J., 2020. Geological seabed stability model for informing Irish offshore renewable energy opportunities. *Adv. Geosci.* 54, 55–65. <https://doi.org/10.5194/ageo-54-55-2020>.
- Pingree, R.D., Griffiths, D.K., 1979. Sand transport paths around the British Isles resulting from M2 and M4 tidal interactions. *J. Mar. Biol. Assoc. U. K.* 59, 497–513.
- Porter-Smith, R., Harris, P.T., Andersen, O.B., Coleman, R., Greenslade, D., Jenkins, C.J., 2004. Classification of the Australian continental shelf based on predicted sediment threshold exceedance from tidal currents and swell waves. *Mar. Geol.* 211, 1–20. <https://doi.org/10.1016/j.margeo.2004.05.031>.
- Ray, D., Leary, P., Livens, F., Gray, N., Morris, K., Law, K.A., Fuller, A.J., Abrahamson-Mills, L., Howe, J., Tierney, K., Muir, G., Law, G.T.W., 2020. Controls on anthropogenic radionuclide distribution in the sellfield-impacted eastern Irish sea. *Sci. Total Environ.* 743, 140765. <https://doi.org/10.1016/j.scitotenv.2020.140765>.
- Robins, P.E., Neill, S.P., Lewis, M.J., Ward, S.L., 2015. Characterising the spatial and temporal variability of the tidal-stream energy resource over the northwest European shelf seas. *Appl. Energy* 147, 510–522. <https://doi.org/10.1016/j.apenergy.2015.03.045>.
- Robinson, I.S., 1979. The tidal dynamics of the Irish and Celtic Seas. *J. Geophys. Res.* 56, 159–197.
- Robinson, K.A., Ramsay, K., Lindenbaum, C., Frost, N., Moore, J., Wright, A.P., Petrey, D., 2011. Predicting the distribution of seabed biotopes in the southern Irish Sea. *Continent. Shelf Res.* 31, S120–S131. <https://doi.org/10.1016/j.csr.2010.01.010>.
- Roe, P.L., 1981. Approximate Riemann solvers, parameter vectors, and difference schemes. *J. Comput. Phys.* 43, 357–372.
- Ruessink, B.G., Walstra, D.J.R., Southgate, H.N., 2003. Calibration and verification of a parametric wave model on barred beaches. *Coast. Eng.* 48, 139–149.
- Tilman, D., 1982. Resource competition and community structure. *Monogr. Popul. Biol.* 17, 296. <https://doi.org/10.4319/lo.1983.28.5.1043>.
- Tiron, R., Gallagher, S., Gleeson, E., Dias, F., McGrath, R., 2015. The future wave climate of Ireland: from averages to extremes. *Procedia IUTAM* 17, 40–46. <https://doi.org/10.1016/j.piutam.2015.06.007>.
- Todd, B.J., Kostylev, V.E., 2011. Surficial geology and benthic habitat of the German Bank seabed, Scotian Shelf, Canada. *Continent. Shelf Res.* 31, S54–S68. <https://doi.org/10.1016/j.csr.2010.07.008>.
- Uehara, K., Scourse, J.D., Horsburgh, K.J., Lambeck, K., Purcell, A.P., 2006. Tidal evolution of the northwest European shelf seas from the Last Glacial Maximum to the present. *J. Geophys. Res.* 111. <https://doi.org/10.1029/2006JC003531>.
- Van Landeghem, K., Besio, G., Niemann, H., Mellett, C., Huws, D., Steinle, L., O'Reilly, S., Croker, P., Hodgson, D., Williams, D., 2013. Amplified sediment waves in the Irish sea (AmSedIS). In: *Marine and River Dune Dynamics – MARID IV*. Bruges, Belgium, pp. 285–290.
- Van Landeghem, K.J.J., Baas, J.H., Mitchell, N.C., Wilcockson, D., Wheeler, A.J., 2012. Reversed sediment wave migration in the Irish Sea, NW Europe: a reappraisal of the validity of geometry-based predictive modelling and assumptions. *Mar. Geol.* 295–298, 95–112. <https://doi.org/10.1016/j.margeo.2011.12.004>.
- Van Landeghem, K.J.J., Uehara, K., Wheeler, A.J., Mitchell, N.C., Scourse, J.D., 2009. Post-glacial sediment dynamics in the Irish Sea and sediment wave morphology: data-model comparisons. *Continent. Shelf Res.* 29, 1723–1736. <https://doi.org/10.1016/j.csr.2009.05.014>.
- Van Rijn, L.C., 1984. Sediment transport, Part I: bed load transport. *J. Hydraul. Eng.* 110, 1431–1456. [https://doi.org/10.1061/\(ASCE\)0733-9429\(1984\)110:10\(1431\)](https://doi.org/10.1061/(ASCE)0733-9429(1984)110:10(1431)).
- Ward, S.L., Neill, S.P., Van Landeghem, K.J.J., Scourse, J.D., 2015. Classifying seabed sediment type using simulated tidal-induced bed shear stress. *Mar. Geol.* 367, 94–104. <https://doi.org/10.1016/j.margeo.2015.05.010>.

- Ward, S.L., Scourse, J.D., Yokoyama, Y., Neill, S.P., 2020. The challenges of constraining shelf sea tidal models using seabed sediment grain size as a proxy for tidal currents. *Continent. Shelf Res.* 205, 104165 <https://doi.org/10.1016/j.csr.2020.104165>.
- Warren, W.P., Keary, R., 1988. The sand and gravel resources of the Irish Sea Basin. In: Sweeney, J.C. (Ed.), *The Irish Sea: A Resource at Risk*, vol. 3. Geographic Society of Ireland Special Publication, pp. 66–79.
- Weber, N., 1991. Bottom friction for wind sea and swell in extreme depth-limited situations. *J. Phys. Oceanogr.* 21, 149–172.
- Wheeler, A.J., Shipboard party, 2009. Irish sea marine assessment (ISMA), CV0926. In: reportCruise Report. 150 pp.
- Wheeler, A.J., Walshe, J., Sutton, G.D., 2001. Seabed mapping and seafloor processes in the kish, Burford, Bray and Fraser banks area, south-western Irish sea. *Ir. Geogr.* 34, 194–211. <https://doi.org/10.1080/00750770109555787>.
- Whitehouse, R., 1998. Scour at marine structures: a manual for practical applications. <https://doi.org/10.1680/sams.26551>.
- Whitehouse, R.J.S., Harris, J.M., Sutherland, J., Rees, J., 2011. The nature of scour development and scour protection at offshore windfarm foundations. *Mar. Pollut. Bull.* 62, 73–88. <https://doi.org/10.1016/j.marpolbul.2010.09.007>.
- Whittington, R.J., 1977. A late-glacial drainage pattern in the Kish Bank area and post-glacial sediments in the Central Irish Sea. In: Kidson, C., Tooley, M.J. (Eds.), *The Quaternary History of the Irish Sea*. Seel House, Liverpool, pp. 55–68.
- Williams, M.E., Amoudry, L.O., Brown, J.M., Thompson, C.E.L., 2019. Fine particle retention and deposition in regions of cyclonic tidal current rotation. *Mar. Geol.* 410, 122–134. <https://doi.org/10.1016/j.margeo.2019.01.006>.
- Wilson, R.J., Speirs, D.C., Sabatino, A., Heath, M.R., 2018. A synthetic map of the north-west European Shelf sedimentary environment for applications in marine science. *Earth Syst. Sci. Data* 10, 109–130. <https://doi.org/10.5194/essd-10-109-2018>.
- Woods, M.A., Wilkinson, I.P., Leng, M.J., Riding, J.B., Vane, C.H., Lopes dos Santos, R.A., Kender, S., De Schepper, S., Hennissen, J.A.I., Ward, S.L., Gowing, C.J.B., Wilby, P. R., Nichols, M.D., Rochelle, C.A., 2019. Tracking Holocene palaeostratification and productivity changes in the Western Irish Sea: a multi-proxy record. *Palaeogeogr. Palaeoclimatol. Palaeoecol.* 532, 109231 <https://doi.org/10.1016/j.palaeo.2019.06.004>.